Title

Single-nucleus resolution mapping of the adult C. elegans and its application to elucidate inter- and trans-generational response to alcohol

Journal

Cell Reports, 42(6)

ISSN

2639-1856

Authors

Truong, Lisa
Chen, Yen-Wei
Barrere-Cain, Rio
et al.

Publication Date

2023-06-01

DOI

10.1016/j.celrep.2023.112535

Peer reviewed

HHS Public Access

Author manuscript

Cell Rep. Author manuscript; available in PMC 2023 October 23.

Published in final edited form as:

Cell Rep. 2023 June 27; 42(6): 112535. doi:10.1016/j.celrep.2023.112535.

Single-nucleus resolution mapping of the adult *C. elegans* and its application to elucidate inter- and trans-generational response to alcohol

Lisa Truong[1,8], **Yen-Wei Chen**[2,8], **Rio Barrere-Cain**[3], **Max T. Levenson**[2], **Karissa Shuck**[3], **Wen Xiao**[4], **Eduardo da Veiga Beltrame**[5], **Blake Panter**[3], **Ella Reich**[3], **Paul W. Sternberg**[5], **Xia Yang**[6], **Patrick Allard**[2,3,7,9,*]

[1]Human Genetics Graduate Program, UCLA, Los Angeles, CA 90095, USA

[2]Molecular Toxicology Inter-Departmental Program, UCLA, Los Angeles, CA 90095, USA

[3]Institute for Society & Genetics, UCLA, Los Angeles, CA 90095, USA

[4]Department of Microbiology, Immunology, and Molecular Genetics, UCLA, Los Angeles, CA 90095, USA

[5]Biology and Biological Engineering, California Institute of Technology, Pasadena, CA 91125, USA

[6]Integrative Biology and Physiology Department, UCLA, Los Angeles, CA 90095, USA

[7]Molecular Biology Institute, UCLA, Los Angeles, CA 90095, USA

[8]These authors contributed equally

[9]Lead contact

SUMMARY

Single-cell transcriptomic platforms provide an opportunity to map an organism's response to environmental cues with high resolution. Here, we applied single-nucleus RNA sequencing (snRNA-seq) to establish the tissue and cell type-resolved transcriptome of the adult *C. elegans* and characterize the inter- and trans-generational transcriptional impact of ethanol. We profiled the transcriptome of 41,749 nuclei resolving into 31 clusters, representing a diverse array of adult cell types including syncytial tissues. Following exposure to human-relevant doses of alcohol, several germline, striated muscle, and neuronal clusters were identified as being the most transcriptionally impacted at the F1 and F3 generations. The effect on germline clusters was confirmed by

*Correspondence: pallard@ucla.edu.

AUTHOR CONTRIBUTIONS

L.T., R.B.-C., K.S., W.X., M.T.L., B.P., and E.R. performed biological experiments and corresponding analyses; Y.-W.C. performed bioinformatic analyses; P.A. and X.Y. supervised experiments; P.A. and X.Y. supervised analyses; E.d.V.B. devised a visualization approach that assisted cell-type assignment and cluster identification, which P.S. supervised; and L.T., R.B.-C., M.T.L., Y.-W.C., X.Y., and P.A. wrote the manuscript.

DECLARATION OF INTERESTS

The authors declare no competing interests.

SUPPLEMENTAL INFORMATION

Supplemental information can be found online at https://doi.org/10.1016/j.celrep.2023.112535.

phenotypic enrichment analysis as well as by functional validation, which revealed a remarkable inter- and trans-generational increase in germline apoptosis, aneuploidy, and embryonic lethality. Together, snRNA-seq represents a valuable approach for the detailed examination of an adult organism's response to environmental exposures.

In brief

Truong et al. apply single-nucleus RNA-seq to profile the transcriptome of the adult *C. elegans* in response to ethanol exposure across generations. They demonstrate the utility of snRNA-seq for studying the asymmetrical inter- and trans-generational effects of environmental cues on different cell types in *C. elegans*.

Graphical abstract

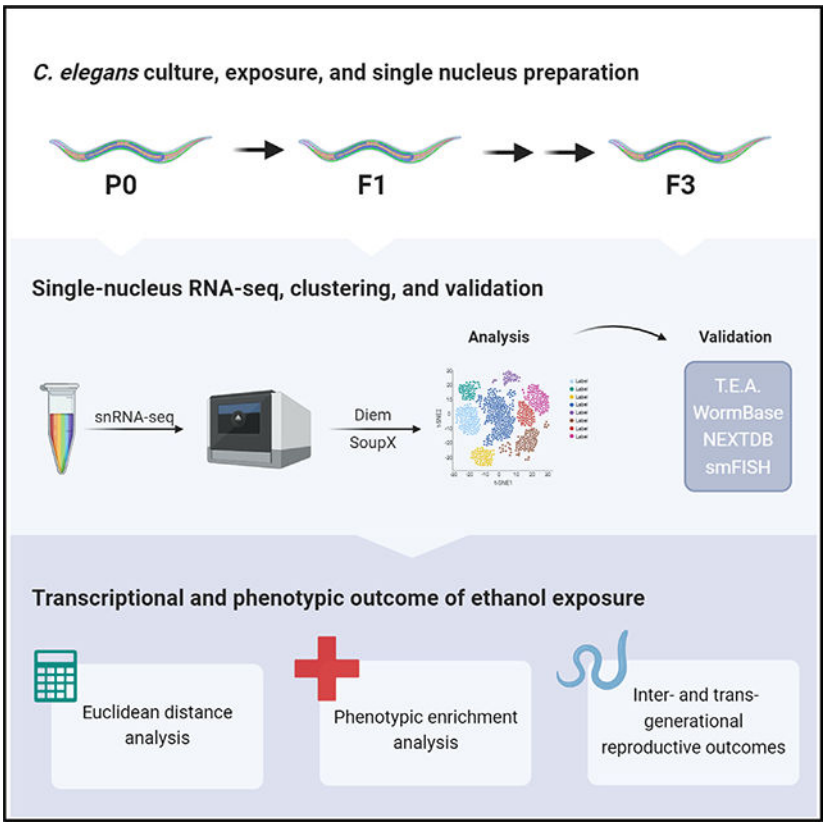

INTRODUCTION

In mammals, *in utero* exposure to alcohol is associated with an array of well-characterized morphological, neurological, and reproductive deficits in the F1 progeny that are grouped into symptoms of fetal alcohol spectrum disorders (FASDs).[1] The plurality of the conditions associated with FASDs reflects the variety of organ systems and processes showing structural and functional anomalies following prenatal alcohol exposure, such as the reproductive system, the central nervous system, craniofacial morphogenesis, and the heart, kidney, liver, and gastrointestinal systems (reviewed in Caputo et al.[2] and La Vignera et al.[3]).

However, while *in utero* alcohol exposure clearly impacts the function of multiple organs, a comprehensive assessment of all organs, tissues, and cell types that are the most affected by alcohol remains lacking.[4]

In addition to impacting the health of the F1 progeny, mounting evidence in various model systems, such as mice, rats, *Drosophila*, and *C. elegans*, indicates that at least some exposure-related adverse reproductive and neurobehavioral features also extend beyond the F1 and are detectable in the F3 progeny.[5–8] For instance, a rat model of late gestational ethanol exposure demonstrated that not only F1 but also F2 and F3 individuals show an average 50% increase in ethanol intake.[9] Fetal alcohol exposure is also associated with altered stress and immune responses associated with gene expression and epigenetic changes.[7,10] Notably, the impact of prior exposure to alcohol on the use of alcohol and other substances in subsequent generations is observed in the broader context of several established multi- and trans-generational models in which various cognitive, behavioral, or physical endpoints are altered (reviewed in Lam et al.[11] and Yoh et al.[12]).

C. elegans is a simplified but highly advantageous model for studying the effects of alcohol and is the most used invertebrate species for modeling FASD (reviewed in Patten et al.[13]). Direct exposure to ethanol causes a variety of dose- and duration-dependent outcomes similar to those elicited in mammals such as growth and fertility impairments, neuro-depressive effects, increased alcohol preference, disinhibition, and withdrawal, all supported by the involvement of similar cellular and neurological pathways.[14–18] The *C. elegans* genome is also equipped with the conserved gene families of alcohol and aldehyde dehydrogenases that provide the main metabolic activity toward ethanol, which is first processed into acetaldehyde and subsequently into acetate.[19] Finally, its reproductive system, with two gonads opening into a common uterus where embryos initiate their development, provides a window for *in utero* exposure to alcohol.

Recently, the combination of single-cell RNA sequencing (scRNA-seq) technologies and the tractability of the model organism *C. elegans*, with its well-established differentiation lineages and timing, has enabled the layering of transcriptional data with developmental events at both embryonic and larval (L2) stages, as well as the mapping of the entire nervous system.[20–22] This has led to the identification of gene expression changes that track the development of 502 preterminal and terminal cell types in embryos[21] and the characterization of 27 distinct cell types at larval stages.[20] Furthermore, we and others have shown that *C. elegans* is also a powerful model for the study of multi- and trans-generational responses to environmental stimuli.[23–28] However, single-cell transcriptomic approaches have yet to be applied to the characterization of environmental exposures, including alcohol, at the whole-organism level and across generations.

Here, we used RNA-seq from single nuclei to maximize the isolation of diverse cell types, including from the approximately 30% of all somatic cells that are polyploid and from the mostly syncytial adult germline.[29,30] We applied this approach to examine the transcriptional impact of parental (P0) exposure to two physiologically relevant doses of ethanol on the F1 offspring (inter-generational exposure) as well as on the F3 generation (trans-generational exposure). We show that single-nucleus RNA-seq (snRNA-seq) identifies numerous distinct

cell types that resolve into well-characterized cellular and functional identities. We also demonstrate that this powerful method can provide insights into the effect of inter- and trans-generational exposure to ethanol at tissue and cell type-specific resolution and identify the cells and molecular pathways that are most impacted by such exposures.

RESULTS

snRNA-seq identifies a wide array of defined cell types in the adult *C. elegans*

Intact nuclei were isolated from adult *fog-1(q253) C. elegans* raised at the restrictive temperature of 25°C.[31] Since the focus of our study was on the characterization of adult tissue responses to ethanol, this sperm-defective strain was used to prevent self-fertilization and the crowding of our snRNA-seq data with embryonic cell types (see STAR Methods). Worms were synchronized and allowed to grow to day 1 of adulthood before mechanical nuclear extraction (Figure 1A). Nuclei concentration was determined using flow cytometry, and nuclear integrity was assessed by high-resolution microscopy. snRNA-seq library preparation was performed using the 10× Genomics Chromium system, followed by 50 paired-end sequencing on the Illumina Novaseq 6000 platform. In total, we generated transcriptomic data for 81,267 nuclei, each with more than 500 transcripts derived from 31 groups collected in 5 distinct batches. On average, 2,181 unique molecular identifiers (UMIs) and 992 genes were detected per nucleus with high sequencing depth (90.3% average sequencing depth) (Figure S1).

The snRNA-seq reads were demultiplexed and aligned to the ENSEMBL ce10 *C. elegans* transcriptome to generate gene expression matrices using CellRanger (10× Genomics) (see STAR Methods). To mitigate the inclusion of debris-contaminated droplets and to correct for ambient RNA contamination, we also applied DIEM[32] and SoupX,[33] respectively. DIEM identifies and removes droplets containing high levels of extranuclear RNA through modeling semi-supervised expectation maximization and outperforms other methods in snRNA-seq.[32] We then combined DIEM with SoupX, which models contamination levels of snRNA-seq with ambient RNA and corrects expression for the remaining droplets. Using these stringent pipelines, we retained transcriptomic data from 41,749 droplets representing a median of 1,627 UMIs and 1,007 genes. A total of 31 discrete clusters were identified following batch/group effect correction by canonical correlation analysis (CCA) in Seurat v.3 followed by Louvain clustering algorithm.[34,35] Log-normalized expression levels in t-distributed stochastic neighbor embedding (t-SNE) plot projections were used to visualize cell clusters in two dimensions, and dot heatmaps were used to visualize marker expression across different cell types (Figures 1B and 2). The full dataset for cluster-resolved gene expression in each of the 31 clusters at false discovery rates (FDRs) <0.05 is compiled in Data S1.

To facilitate unbiased cluster identification, gene enrichment (FDR < 0.05) in each cluster was used to mine the tissue enrichment, Gene Ontology, and phenotype enrichment modules of WormBase[36] (Figure 1A). The output from these modules was cross-referenced with *in situ* expression data of the top enriched transcripts using the Nematode Expression Pattern Database (NEXTDB; https://nematode.nig.ac.jp/). Comprehensive information for all 31 clusters that include top enriched and depleted genes, the 3 WormBase modules

outputs, and representative examples from NEXTDB are presented in a dashboard (Data S2). Examples are shown in Figure 2 alongside relative expression levels of several known markers of each cell type showing notably high concordance. For example, cluster 23 is the only cluster showing a high expression level of the germline-specific transcript *tra-2*,[37] the meiotic-specific endonuclease *spo-11*, and the synaptonemal complex components *syp-1* and *syp-3* (as well as *syp-2* and *syp-4*, which are not depicted here).[38,39] In the adult *C. elegans* germline, the expression of *tra-2* is restricted to the most distal section of the germline and overlaps with that of the Notch signaling target *sygl-1*.[40,41] To test whether cluster 23 could correspond to the distal germline, we confirmed *sygl-1* expression by small-molecule fluorescence *in situ* hybridization (smFISH) as previously described[41] and compared its expression with its tSNE distribution (Figure S2). As expected, *sygl-1* showed a high expression level in the region corresponding to cluster 23 with some expression in other germline clusters, which matched its smFISH distribution and published data,[40] indicating that cluster 23 likely corresponds to the distal germline.

Similarly, cluster 3 specifically expresses all known markers of the spermatheca such as *fkh-6*, *ule-3*, *ule-5*, and also *ZK813.7*.[42,43] Marker analyses also revealed that subregionalization within clusters is apparent. For example, the three GABAergic neuron markers *unc-25*, *unc-46*, and *unc-47*[44] resolve in one section of cluster 11 (Figure 2), which also expresses markers of cholinergic neurons (e.g., *cha-1* and *cho-1*).[45] Also of note, based on WormBase's tissue enrichment analysis (TEA), several tissue and cell types are represented by multiple clusters (e.g., the germline represented by 6 clusters, the intestine and epithelial system, represented by 3 clusters each) (Data S2), likely reflective of the cellular heterogeneity underlying the composition of those tissues. Only clusters 0 and 9 (2/31) showed a lack of concordance between TEA, Gene Ontology (GO), and *in situ* data, precluding assignment of a clear identity. All snRNA-seq data can be accessed at https://singlecell.broadinstitute.org/single_cell/study/SCP922/single-nucleus-resolution-mapping-of-the-adult-c-elegans-and-its-application-to-elucidate-inter-and-trans-generational-response-to-alcohol (also see data and code availability).

snRNA-seq reveals broad impacts of inter-generational exposure to ethanol

We applied snRNA-seq to identify the organism-wide transcriptional outcome of a parental 48 h (L4 to end of day 1 of adulthood) exposure to two concentrations of ethanol (0.05% and 0.5%) or water control on the F1 adult progeny. These doses were chosen to circumscribe the wide range of human blood alcohol concentrations associated with low (0.05%) or high (0.5%) alcohol use.[46] We first assessed the reproducibility of our approach by calculating the Pearson's correlation coefficient between either each of three control samples vs. all ethanol-treated samples or each of three ethanol-treated samples vs. all control samples. The median r coefficient of all clusters was high, ranging from 0.66 to 0.80 based on ethanol concentration and generation (Figure S3A), indicating a good agreement between ethanol-exposed samples and controls across biological repeats.

To assess the impact of ethanol, we first compared cell-type proportion in the F1 following parental ethanol exposure and observed that broadly similar cluster distributions

were observed across all treatment conditions (Figure S3B). However, we observed a significant number of differentially expressed genes (DEGs) (FDR < 0.05) between treatment conditions (Figure 3A). Across all F1 clusters from the 0.05% ethanol-exposure condition, we identified a total of 1,223 DEGs, including 583 uniformly upregulated DEGs, 520 uniformly downregulated DEGs, and 120 DEGs that were differentially up- or downregulated in cluster-specific ways (i.e., upregulated in some clusters but downregulated in other clusters) (Table S2). Surprisingly, compared with 0.05%, exposure to the higher ethanol concentration of 0.5% resulted in fewer DEGs identified at the F1 (Table S3) with a total of 948 DEGs, including 430 uniformly upregulated DEGs, 407 uniformly downregulated DEGs, and 111 up- and downregulated DEGs (Figure 3A).

GO of the union of all DEGs revealed the enrichment of some functional categories that align with alcohol metabolism such as the GO category “carboxylic acid metabolic process” driven by the presence in the DEG list of several aldehyde dehydrogenases (Tables 1 and S4), which catalyze the final step of ethanol metabolism from acetaldehyde into acetate. However, a major target of ethanol across exposure conditions and clusters is the translation machinery, as exemplified by the deregulation of many ribosomal components and representing 5 of the top 10 GO categories, including the top 3 (Table S4). The inhibition of translation and the downregulation of genes encoding ribosomal subunits are well-described and conserved impacts of alcohol exposure *in vitro* and in a variety of species from bacteria to humans.[47–52] In addition, reproductive pathways were among the most affected across exposure conditions at the F1, such as “gamete generation,” “germ cell development,” and “embryo development ending in birth or egg hatching” pathways (Table S4).

snRNA-seq reveals tissue-specific DEGs from inter-generational (P0 to F1) exposure to ethanol

Next, we conducted cluster-specific DEG analysis to investigate cell type-specific effects at the F1. Cluster-resolved DEG analysis indicated clearly distinct transcriptional responses to parental ethanol exposure between cell types. While some genes were consistently upregulated (*atp-6*, *nduo-6*) or downregulated (*vit-5*) across all clusters between ethanol and water treatment, most DEGs showed cell type-specific restriction as highlighted by the low overlap of the top DEGs per cluster (Figure S4; Tables S2 and S3). To rank order the F1 clusters by sensitivity to ethanol exposure, we employed a Euclidean distance analysis,[53,54] which estimates the degree of transcriptomic shifts between exposure and control groups (see STAR Methods). Several clusters (1, 15, and 30) with an assigned germline identity based on TEA, GO, phenotype enrichment analyses, and NEXTDB (Data S2) showed some of the largest degrees of transcriptomic shifts at the F1 generation under the 0.5% ethanol exposure condition (Figure 3B). Other cluster categories that appeared most affected included clusters related to muscle function such as clusters 2 and 17, both carrying striated muscle cell identity. The degree of transcriptomic shift was much less pronounced following 0.05% ethanol exposure compared with 0.5% ethanol, suggesting a dose-dependent transcriptomic response across cell types.

We hypothesized that while most DEGs are cell-type specific, genes implicated in ethanol metabolism may show a more uniform response across clusters. Thus, we investigated the expression of genes involved in ethanol metabolism, including 3 distinct alcohol dehydrogenase (*sodh-1*, H24K24.3, ZK829.7) and 10 aldehyde dehydrogenases (*alh-3*, *−4*, and *−7* through *−13*) whose expression was detectable in our datasets (Figure S5). Contrary to our expectations, of the 13 genes examined, only 5 showed significant changes in expression (FDR < 0.05) and did so in a cluster- and dose-dependent fashion. For example, *sodh-1* was upregulated in clusters 13 and 18 under the 0.05% exposure condition but was downregulated in clusters 2 and 27 at 0.5%. Notably, the cell types showing the highest increase in ethanol metabolism genes were not the cell types that were the least sensitive to ethanol, and vice versa, suggesting that the upregulation of ethanol metabolism genes in the F1 does not protect a tissue from the inter-generational impact of exposure (compare Figures 3B and S5).

At the F1, the majority of the clusters reaching statistical significance (FDR < 0.05) after 0.5% ethanol exposure in our Euclidean distance analysis displayed a germline identity, e.g., clusters 1, 12, 15, 23, and 30. Thus, we next examined whether reproduction-related phenotypes were significantly overrepresented in our dataset. We analyzed the top 10 most shared WormBase phenotypes across cell types with significantly altered Euclidean distance and identified several phenotypic terms related to reproduction (e.g., “diplotene region organization variant,” “pachytene region organization variant,” “germ cell compartment expansion variant”) that are mildly upregulated in germline cluster 1 but strongly and uniformly downregulated in germline cluster 12 (Figure 4A). We also examined whether the DEGs across the sensitive cell types were enriched in specific phenotypes by comparing the DEGs’ phenotype enrichment outcome with all WormBase phenotypes. This analysis revealed that our dataset has a significantly higher proportion of phenotypes related to reproductive system development, cellular development, and morphology categories among both treatment groups (Figure 5A).

Since the germline appears to be a major target for ethanol at the F1 and F3 generations, we validated the magnitude and directionality of the transcriptional impact of ethanol exposure in that tissue. For example, in our snRNA-seq dataset, *tra-2* showed a significant downregulation of its expression in cluster 23 in the F1 under 0.5% ethanol exposure (Figure 3D; Table S3; 0.60-fold change, adjusted p value = 0.003). We performed smFISH in dissected F1 germlines followed by quantification using FISH-quant (Figures 3F–3I). We observed a congruent 0.47-fold downregulation of the *tra-2* level ($p < 0.05$). Conversely, at the F3 under the 0.5% ethanol-exposure condition, *mex-3* was significantly upregulated in our snRNA-seq dataset in germline cluster 12 (Figure 3E; Table S6; 1.58-fold change, adjusted p value = 0.008). Cluster 12 also carries a meiotic germline identity based on GO enrichment (Data S2). smFISH indicated an upregulation of *mex-3* in the mid-pachytene region of F3 *C. elegans* gonads (2.19-fold, $p < 0.001$). We also examined the impact of ethanol by smFISH on two additional transcripts in non-germline cell types at different concentrations and generations, i.e., in coelomocytes (*dig-1* in cluster 28) at the F1 following 0.5% ethanol exposure and in neurons (*egl-3* in cluster 11, which includes GABAergic and cholinergic neurons) at the F3 following 0.05% ethanol exposure. In each case, the directionality of the impact of ethanol was consistent between the snRNA-seq and

smFISH data, although with varied p values ($p \leq 0.005$ and $p = 0.19$ for *dig-1* and *egl-3*, respectively, Welch's t test) (Figure S6).

Together, these results indicate a strong inter-generational impact of alcohol in *C. elegans* on a variety of cell types including those that belong to the germline.

Trans-generational (P0 to F3) impact of ethanol

We extended our snRNA-seq approach to the F3 generation to capture the trans-generational effect of P0 exposure to ethanol. Similarly to the F1, no overt impact on cell-type distributions was observed (Figure S3A). Across all clusters at the F3 stemming from a P0 0.05% ethanol exposure, a total of 798 unique DEGs—366 unique upregulated DEGs, 369 unique downregulated DEGs satisfying an FDR <0.05, and 63 DEGs that were differentially up- or downregulated in cluster-specific ways—were found (Figure 3A; Table S5). For 0.5% ethanol, a total of 918 unique DEGs were identified comprising 402 unique upregulated DEGs, 422 unique downregulated DEGs satisfying an FDR <0.05, and 94 DEGs that were differentially up- or downregulated in cluster-specific ways (Figure 3A; Table S6).

GO analysis of all F3 DEGs revealed the enrichment of some functional categories that align with alcohol metabolism. These were exemplified by GO categories such as "carboxylic acid metabolic process," "drug metabolic process," and "small molecule catabolic process," driven in part by the presence in our DEG list of alcohol dehydrogenase genes, *sodh-1* and *hphd-1*, which catalyze the first step of ethanol metabolism from ethanol to acetaldehyde, as well as aldehyde dehydrogenase genes, *alh-8* and *alh-13*, which catalyze the second step of ethanol metabolism from acetaldehyde into acetate, in both exposure groups compared with water at the F3 (Tables 1 and S4). Other highly enriched GO terms were "structural molecule activity," "cytoskeleton organization," "translation," and reproductive GO categories "embryo development ending in birth or egg hatching" and "sexual reproduction."

Cell type-specific trans-generational response to ethanol

Next, we conducted cluster-specific DEG analysis to investigate ethanol's trans-generational effects. While the majority of top DEGs at the F1 were upregulated, in comparison, the majority of the top DEGs found at the F3 were downregulated, especially at the 0.5% ethanol-exposure condition (Figure S7). These top DEGs showed remarkable cell-type specificity as highlighted by their low overlap across clusters. We assessed the sensitivity of individual clusters by measuring their Euclidean distance (Figure3C). Notably, compared with the F1 results, more clusters reached the cutoff of FDR <0.05 from 0.5% exposure at the F3. While changes in the relative order of the clusters were observed between F3 and F1, several germline clusters showed some of the largest transcriptomicshifts,includingcluster1,whichremainedasthecluster that is the most transcriptionally affected by ethanol (Figure 3C).

The examination of F3 DEGs through the WormBase phenotype enrichment tool revealed a strong alteration of different phenotypes under the 0.5% ethanol-exposure condition, albeit in a less uniform fashion across clusters (Figures 4B and 5B). The pachytene region organization variant phenotype was downregulated in cluster 1 but not in other germline

clusters, suggesting a lasting but weakened impact of ethanol exposure at the F3. A comparison of phenotype proportion between our dataset and all phenotypes revealed a persistent enrichment in the F3 of the phenotypic categories described in the F1 including a higher proportion of reproductive system development variants at 0.5% ethanol. By contrast to the F1, no phenotypic category reached significance under the 0.05% ethanol-exposure condition, confirming the weakened impact of ethanol at the F3.

Functional outcomes of ethanol's inter- and trans-generational transcriptional impacts

The presence of several germline clusters among the most transcriptionally impacted clusters as well as the enrichment of some reproductive phenotypes at the F1 and F3 suggested that ethanol exposure may have a significant functional impact on reproduction at these generations. To test this hypothesis, we measured three hallmarks of reproductive health in *C. elegans*: germline apoptosis by acridine orange staining,[55] the missegregation of chromosomes during meiosis by monitoring the segregation of the X chromosome,[56] and embryonic lethality through plate phenotyping.[57,58] All three reproductive measures were significantly increased at either 0.05% or 0.5% ethanol exposures in the F1 and in the F3 compared with the water control, remarkably, with no consistent dose-response relationship (Figure 6). Analysis of germline apoptosis through acridine orange staining revealed a 2-fold increase in the number of apoptotic nuclei per gonad in F1 worms who were exposed to 0.05% ethanol at the P0 ($n = 5$, $p < 0.05$) and a 2.7-fold increase in those who were exposed to 0.5% ethanol ($n = 5$, $p < 0.0001$) when compared with water. Similarly, at the F3, a 1.9-fold increase for both ethanol-exposure conditions was observed when compared with water ($n = 4–5$, $p < 0.001$). Next, we monitored chromosome segregation through the segregation of the X chromosome using a strain carrying the *Pxol-1::gfp* reporter.[56,59] Chromosomes that fail to properly segregate during meiosis result in embryos with aneuploidies.[39] Here, we monitored aneuploidy via the incidence of male (XO) embryos, which are caused by missegregation of the X chromosome and marked by the expression of the male-specific *xol-1* promoter driving GFP expression. Analysis at the F1 identified a significant increase in the incidence of GFP-positive embryos for both ethanol-exposure conditions when compared with water, with a 2.6-fold increase in the proportion of worms with at least one GFP-positive embryo at 0.05% ethanol exposure ($n = 6–7$, $p < 0.01$) and a 2.8-fold increase at 0.5% ethanol exposure ($n = 6–7$, $p < 0.01$). The incidence of GFP-positive embryos further increased at the F3 with a 4-fold increase at 0.05% ethanol exposure ($n = 6–7$, $p < 0.01$) and a 4.3-fold increase at 0.5% ethanol exposure ($n = 6–7$, $p < 0.001$). Finally, plate phenotyping assay revealed, at the F1, a 3.8-fold increase in embryonic lethality for worms ancestrally exposed to 0.05% ethanol compared to water ($n = 4$, 3 worms per condition per repeat, $p < 0.001$) and a 4.9-fold increase for those exposed to 0.5% ethanol exposure compared to water ($n = 4$, 3 worms per condition per repeat, $p < 0.0001$). In comparison at the F3, a 2-fold increase for 0.05% ethanol exposure ($n = 10$, 2–3 worms per condition per repeat, $p < 0.01$) and a 2.5-fold increase for 0.5% ethanol exposure ($n = 10$, 2–3 worms per condition per repeat, $p < 0.0001$) were observed. Together, these results indicate a profound impact of inter- and trans-generational alcohol exposure on the nematode's reproductive function congruent with the outcome of our snRNA-seq analysis.

DISCUSSION

We developed an snRNA-seq approach in the adult *C. elegans* hermaphrodite nematode and identified a substantial number of transcriptionally distinct cell types. By applying this approach to the study of the inter- and trans-generational impacts of ethanol exposure, we also demonstrate its utility in achieving a nuanced understanding of transcriptional responses to environmental cues.

We circumvented some of the drawbacks associated with single-nucleus approaches by employing multiple data clean-up pipelines to identify and remove debris-contaminated droplets and spurious signal from ambient RNA, a common artifact of snRNA-seq.[32,33] This stringent approach removed approximately half of all droplets but still generated a robust number of UMIs and genes per nucleus when compared with other studies. Our approach also generated a number of clusters corresponding to cell types previously underrepresented in single-cell RNA-seq studies in *C. elegans* because of their lack of cellularization, e.g., meiotic stages of the germline and hypodermal cells.

The application of our snRNA-seq approach to the study of ethanol's response across generations highlighted the complexity of organisms' response to environmental cues. This aspect was exemplified by the diversity and specificity of GO categories by clusters (Table S4) and by the low degree of overlap of top DEGs between clusters (Figures S4 and S7). Because of their high ranking in the Euclidean analysis in both F1 and F3 generations, several tissue types stood out as being particularly affected by ethanol: the muscle system, neurons, and the germline. The direct impact of alcohol on skeletal and cardiac muscle cells is well described and a common outcome of chronic alcohol use.[60–62] An inter-generational effect of prenatal alcohol exposure on the musculature and muscle function has also been demonstrated and is referred to as fetal alcohol myopathy.[63,64] Interestingly, a proposed mechanism for this induced muscle cell dysfunction is an alteration of protein synthesis,[65,66] which is represented by several GO categories (e.g., "peptide metabolic process," "peptide biosynthetic process," "translation") in our DEG pathway analysis (Table S4). Supplementation of amino acids to facilitate translation processes might be tested as a method of improving the impact of ethanol on the F1 muscle cells. The mechanisms of trans-generational impact of alcohol on F3 musculature, however, is unclear and has not been previously described.

Similarly, cluster 11, which comprises GABAergic (e.g., *unc-25*$^{+}$) and some cholinergic neurons (e.g., *cha-1*$^{+}$), is also identified as being significantly altered by 0.5% ethanol at the F1 and F3. Interestingly, GABAergic neurons are also a well-known target of direct and inter-generational alcohol exposure in which alcohol leads to overstimulation of the GABA system, leading to dampening of neuronal excitability.[67–70] To a lesser extent, cholinergic signaling has also been implicated in the inter-generational impact of ethanol on the nervous system.[71–73] Since in *C. elegans*, direct alcohol exposure is associated with a deregulation of cholinergic signaling and locomotory behavior,[16,74] it will be important to also investigate the role of GABA signaling and its interaction with cholinergic signaling in regulating locomotion not only in a direct exposure paradigm but also across generations.

Germline clusters were ranked the highest in the Euclidean distance analysis at the F1 and F3 generations. We therefore focused our validation experiments on the germline and reproduction. Direct ethanol exposure has been known to cause aneuploidy in mammalian germ cells for many years[75–77]; however, whether these effects extend to the F1's germline has remained uncertain. Our results clearly indicate that in *C. elegans*, both low and high concentrations of ethanol have a profound impact on reproductive function (germ cell apoptosis, aneuploidy, embryonic lethality) and that these impacts extend trans-generationally. We have previously demonstrated that the trans-generational reproductive effects of the environmental chemical bisphenol A requires the alteration of the repressive histone marks H3K9me3 and H3K27me3.[23,25] Inter-generational alcohol exposure, on the other hand, has been shown to lead to histone hyperacetylation through the metabolism of ethanol into acetate.[78] Thus, it is plausible that alcohol's inter- and trans-generational outcomes described here may be initiated by the hyperacetylation of histone in the germline. Finally, while we validated ethanol's impacts on several DEGs by smFISH in the germline, a more comprehensive DEG validation in other tissues will be needed as well as a comparison with cell type-specific inter- and trans-generational ethanol transcriptional outcomes in mammalian models when such data become available.

Limitations of the study

Our approach nonetheless has several limitations. By working in a *fog-1* mutant background, we were not able to identify sperm cells, highlighted by the absence of expression of canonical sperm markers in our dataset. This was considered a necessary trade-off to avoid the production of embryos and the crowding of snRNA-seq data with a large and diverse number of embryonic cell types. While it is possible that *fog-1*'s absence alters the transcriptional landscape of the germline, *fog-1(q253)* was chosen specifically because of the normal morphology and staging of the hermaphrodite germline in the *fog-1* mutant background.[31] The temperature sensitivity of the *fog-1(q253)* allele, necessary for strain maintenance, requires a shift to the non-permissive temperature of 25 °C at the generation of collection that may cause a transcriptional effect on its own.[28] In our experimental design, all samples, exposed and controls, were equally temperature shifted, thus correcting for additive (but not synergistic) effects between temperature and ethanol exposures.

For a small number of clusters, tissue enrichment analysis did not delineate a clear cell-type identity (2/31 clusters) either representing cell types with mixed identities or cell types for which other clustering methods would be beneficial. Nonetheless, the majority of clusters bore a distinctive tissue identity not only corroborated by GO and phenotype enrichment analyses but also by the tissue-specific *in situ* expression pattern of genes showing the highest degree of cluster specificity. Additionally, the number of clusters obtained is lower than the number of cell types that could be expected (e.g., 118 neuronal classes have been identified with 146 different molecular profiles[79]). There are several potential reasons underlying this discrepancy: while we chose to perform single-nucleus extraction to avoid isolation bias, the mechanical disruption of the worms may lead to undersampling of some cell types. While this is a possibility, the dashboard analysis indicates that all tissue types are represented. Thus, any undersampling would be of a more discrete nature than at the tissue level. The overlapping expression profiles of distinct cell types combined with the use of

the Louvain algorithm within Seurat is likely a contributor to the grouping of distinct cell types into shared clusters. Cluster 11 is representative of this: while GABAergic neurons are fully embedded within cluster 11, they group at one edge of cluster 11, suggesting that other neuronal types that are not GABAergic form the remaining part of the cluster. This is supported by the restricted expression of the choline transporter *cho-1* in cluster 11, although in a distinct subsection of the cluster. The resolution parameter chosen from FindClusters() within Seurat leads to a minimal overlap of the known cell-type markers that were examined (see Figure 2); however, it is possible to further increase the number of clusters by altering the resolution parameter within Seurat based on user preference and study goals.

Together, the application of snRNA-seq to the adult *C. elegans* represents a valuable approach for the identification and simultaneous characterization of multiple cell types in the nematode in different environments.

STAR★METHODS

RESOURCE AVAILABILITY

Lead contact—Further information and requests for resources and reagents should be directed to and will be fulfilled by the lead contact, Dr. Patrick Allard (pallard@ucla.edu).

Materials availability—This study did not generate any new unique reagents.

Data and code availability

- All raw data is accessible on NCBI's Gene Expression Omnibus (GEO), at: https://www.ncbi.nlm.nih.gov/geo/query/acc.cgi?acc=GSE208229.
- This paper does not report original code.
- Any additional information required to reanalyze the data reported in this paper is available from the lead contact upon request.

EXPERIMENTAL MODEL AND SUBJECT DETAILS

The strain JK560 *fog-1(q253)* was used for sequencing and single molecule fluorescence *in situ* hybridization (smFISH) experiments. N2 (wild type) worms were used for embryonic lethality and acridine orange apoptosis experiments. The strain TY2441 (*Pxol-1::gfp*; *rol-6(pRF4)*) was used for X chromosome aneuploidy experiments. Worms were cultured on standard nematode growth medium (NGM) plates streaked with single colony OP50 *E. coli* and maintained at 20°C. The generation of worms to be collected for single-nucleus analysis was moved to 25°C at the L1 stage and grown at 25°C for 48 hours until the beginning of day 2 of adulthood. To collect L1 larvae from the F1 generation, worms were synchronized by bleaching P0 gravid adults and having their F1 embryos subsequently grown for 16 hours at 20°C at which time all F1 were at the L1 stage. To collect L1 larvae from the F3 generation, the L1 larvae were collected through filtration using a 10μm nylon mesh filter (EDM Millipore NY1102500 and EDM Millipore SX00025000) which only allows L1 stage worms to pass through. L1 worms for both generations were kept for 48 hours at 25°C and then washed with five rounds of M9 buffer and centrifuged at 1,300g for 1 minute to

pellet worms between each wash. After the final wash, worms were spun in a rotator with 1mL of M9 for 30 minutes to remove OP50 from the worms' gut. The worms were then allowed to settle by gravity for 5 minutes and the final compact worm pellet volume was adjusted to 30μL. The aforementioned strains were obtained from the *C. elegans* Genetics Center (CGC): JK560 *fog-1(q253)* I; TY2441 *yls34* (*Pxol-1::gfp+rol-6 (pRF4))* (obtained by crossing *him-8(e1489)* out of TY2431); N2: wild-type.

METHOD DETAILS

***C. elegans* ethanol exposure and culture expansions—**For ethanol exposures, a population of gravid adult worms was bleached. The embryos obtained were plated on standard OP50 seeded NGM plates and allowed to grow to the L4 stage (approximately 50 hours post bleaching). Nematodes were exposed for 48 hours in liquid culture containing M9 buffer solution, standard OP50 bacteria (10 mg/mL), and ethanol at a final concentration of 0.05% or 0.5% in 15mL conical tubes. Following the liquid exposure, the progeny of the exposed P0 generation were obtained using gravid adult bleaching. The synchronized F1 egg population was then plated on multiple standard OP50-seeded NGM plates. Half of the plates were grown for 16 hours at 20°C at which time all F1 were at the L1 stage, and these plates were then transferred to 25°C for 48 hours into adulthood before proceeding with single-nucleus dissociation of the F1 generation.

The other half of the plates were grown at 20°C for 4 days or until the plates were filled with F2 L1 larvae. This population was synchronized using a 10μm nylon mesh filter (EDM Millipore NY1102500 and EDM Millipore SX00025000) which only allowed L1 staged worms to pass. The L1 worms were washed twice with M9 and centrifuged at 100g for 1 minute. These L1 worm pellets were plated on fresh OP50-seeded NGM plates and grown at 20°C for 4 days or until the plates were filled with F3 L1 larvae. This population was synchronized using a 10mm nylon mesh filter similar to the F2 population and the F3 L1 plates were transferred to 25°C. Worms were grown for 48 hours at 25°C before proceeding with single-nucleus dissociation of the F3 generation.

Single-nucleus dissociation—All reagents were prepared using RNase free water (Thermo Fisher BP2484100). The FA lysis buffer was made using the following reagents: 50mM HEPES/NaOH pH 7.5, 1mM EDTA, 0.1% Triton X-100, 150mM NaCl, Protease inhibitor 0.5X (Roche 11697498001), RNase inhibitor 0.2U/μL (Thermo Fisher 10777019), and RNase free water and stored at 4°C or on ice. BSA was prepared to a final concentration of 1% in pH 7.4 1X PBS (Thermo Fisher AM9624) using RNAse free water and RNAse free PBS. This solution was filtered using a 0.22μm pressure filter (Thermo Fisher 03-377-26, Thermo Fisher SLGP033RS).

All equipment and reagents were moved to a 4°C cold room and subsequent steps were performed at 4°C. Homogenizers were stored pre-chilled at −20°C when not in use and moved to the 4°C room before starting the extraction. Each Wheaton 1.5mL Dounce homogenizers (Sigma Z378623-1EA) was cleaned using 70% ethanol, RNaseZAP, and RNase free water. Homogenizers were rinsed twice with ethanol, twice with RNaseZAP, and 5 times with 1–2mL of RNase free water.

For both F1 and F3 generations, L1 larvae were grown at 25°C for 48 hours. Adult worms were gently washed off plates with M9 and transferred into 15 mL conical tubes, being careful not to disrupt bacterial lawn. Worms were allowed to settle to the bottom of the conical tube by gravity for 5 minutes before transferring the worm pellet to a sterilized 1.5mL low bind microcentrifuge tube. The worm pellet was then washed 5 times with M9, centrifuging the tubes at 1,300g for 1 minute in between each wash in order to remove bacteria. After washing, worms were placed in 1mL of M9 in a 1.5mL low bind microcentrifuge tube and incubated in a rotator at 20°C for 30 minutes to remove residual OP50 from the worms' gut. These microcentrifuge tubes were then set upright and the worms were allowed to settle by gravity for 5 minutes. The M9 supernatant was discarded and the final compact worm pellet volume was adjusted to 30μL.

The compact 30μL pellet of adult *C. elegans* was transferred to the Dounce homogenizer and 400μL of ice-cold FA buffer was used to rinse any remaining worms from the 1.5mL low bind microcentrifuge tube and added to the homogenizer. Worms were homogenized with 10 strokes of the Dounce homogenizer using a corkscrew motion with a B (tight) pestle. Homogenized worms were transferred to a new low bind 1.5ml microcentrifuge tube and centrifuged at 100g for 1 minute to pellet debris. The supernatant containing the dissociated nuclei was removed using a 1,000μL low bind tip and transferred to a fresh low bind 1.5mL microcentrifuge tube labeled pooled nuclei. 300μL of FA buffer was added to the debris remaining in the first microcentrifuge tube and homogenized using 10 strokes in a corkscrew fashion with an Eppendorf Dounce homogenizer. The newly homogenized sample was then centrifuged at 100g for 1 minute to pellet debris. The supernatant containing the newly dissociated nuclei was pooled with the previously dissociated nuclei and the previous steps with the Eppendorf Dounce homogenizer were repeated once more to further homogenize the sample. In total, worms were homogenized with 30 strokes: 10 strokes with the 1.5mL Wheaton Dounce homogenizer and 20 strokes with the Eppendorf Dounce homogenizer. Between each homogenization step, debris was pelleted at 100g for 1 minute and the supernatant containing the dissociated nuclei was removed and added to a single 1.5mL microcentrifuge tube labeled pooled nuclei. Dissociated nuclei were removed after each set of 10 homogenization strokes to prevent over digestion of nuclei.

After homogenization, the pooled supernatant containing the dissociated nuclei was centrifuged at 100g for 1 minute to pellet any remaining or accidentally transferred debris. The top 900μL of supernatant containing nuclei was transferred to a clean low binding 1.5mL microcentrifuge tube, being careful not to disturb the debris pellet. These pooled nuclei were pelleted at 500g for 4 minutes. After pelleting, approximately 800μL of FA buffer was removed, being careful not to disrupt the nuclei pellet, and the pelleted nuclei were resuspended with 1,000μL of 1% PBS-BSA. The nuclei were again centrifuged at 500g for 4 minutes and 1,000μL of the 1% PBS-BSA supernatant was removed. Lastly, the nuclei pellet was resuspended in 750–850μL of 1% PBS-BSA (final volume was determined by examining the size of the nuclei pellet). After resuspension, the nuclei were filtered using a 40μm Flowmi tip filter (Sigma Aldrich BAH136800040-50EA). Filtered nuclei were transferred to a 1.5mL low retention microcentrifuge tube for FACS sorting or 10X sequencing.

Flow cytometry and FACS—The BD Analyzer Celesta plate reader at the UCLA BSCRC flow cytometry core was used to assess nuclei concentration. 150μL aliquots of filtered nuclei samples were stained with DAPI to determine concentration and integrity. Flow cytometry was done using the Violet 405nm 50mW laser with the slowest flow rate to obtain accurate counts. Nuclei concentration was determined to be between 700 to 1,200 nuclei per microliter. If concentration was too high, filtered nuclei sample was diluted with 1% PBS-BSA. A flat bottom clear 96-well plate was used to assess nuclei concentration.

Library preparation and sequencing—Library preparation was performed by UCLA Technology Center for Genomics & Bioinformatics. Nuclei were isolated into single droplets and barcoded using the 10X Chromium Next GEM single cell 3′ reagent kit. We sequenced using 50bp long paired end reads with the NovaSeq 6000.

Single-nuclei transcriptional analysis—snRNA-seq reads were demultiplexed and aligned to the ENSEMBL ce10 *C. elegans* transcriptome to generate gene expression matrices using CellRanger (10x Genomics). The reference transcriptome was converted to accommodate pre-mRNA alignment by replacing “transcript” to “exon” in annotation GTF file. We first filtered the matrices to exclude low-quality cells or potential doublets using the following criteria: 1) gene number less than 300 or more than 8000, 2) unique molecular identifier (UMI) count less than 500 or more than 20000, 3) mitochondrial RNA percentage > 15% per cell, and 4) ribosomal RNA >20% per cell. After pre-processing, 4694, 16148, 11738, 9169 cells were retained in unexposed, water treatment,0.05% and 0.5% ethanol treatment groups, respectively.

Clustering analysis—R Seurat 3.1.5[34] package was used for normalization, cell type identification, marker identification and batch effect correction of snRNA-seq data using all 31 sample groups. snRNA-seq data was log-normalized. The top 2,000 variable genes were selected as representative features, followed by correcting gene expression with UMI counts, mitochondrial gene percentage and ribosomal RNA percentage for further clustering analysis. Canonical correlation analysis (CCA) was applied across different batches and treatment conditions to mitigate batch effects in cluster identification. Cell clusters were identified from Louvain algorithm.[35] We included all treatment groups for unsupervised clustering since increased cell numbers was shown to increase power in identifying smaller cell types.[81] Cluster specific genes were detected by Wilcoxon Rank Sum test.[82] To reduce biases from treatment in finding markers, only unexposed cells were included unless unexposed groups consist of less than 20% of the cluster of interest. Furthermore, for each cluster, the gene had to be expressed in at least 25% of the cells of the given cluster and there had to be at least a 0.25 log fold change in gene expression compared to other cells. Log-normalized expression levels in t-SNE (t-distributed stochastic neighbor embedding) plot projections were used to visualize cell clusters in two dimensions and dot heatmap were used to visualize marker expression across different cell types. While tSNE clusters were created using all 31 samples, marker genes enriched for each cluster were identified using only the unexposed samples to avoid confounding effects of ethanol.

Differential gene expression and pathway analyses—Monocle[83] pipeline was used to identify DEGs across different cell types, generations, and dose levels. Four different monocle models were created to assess DEGs in F1_0.05, F1_0.5, F3_0.05 and F3_0.5 condition. For each condition (generation and dose level), only cell types with more than 10 cells in each group were included. For genes expressed in more than 20% of cells in each cell type, a negative binomial model was fitted based on raw counts to normalize data, followed by fitting a generalized linear model to retrieve exposure effect with batch effects corrected as follows:

$$Gene\ expression = b1 * batch + b2 * ethanol + b3 * gene\ count + b4 * UMI\ count$$

Batch term is only included in F1_0.05 and F3_0.05 where two batches of water and ethanol 0.05% samples were produced, for F1_0.5 and F3_0.5 condition this term is not used since only water and ethanol 0.5% samples from the same batch were considered. The b2 coefficient obtained was used to estimate exposure effects. Statistical p-value was obtained using a likelihood ratio test against the null model where the exposure term is not included. Significant DEGs were defined as genes with Benjamini & Hochberg corrected FDR < 0.05.[84]

The DEGs were then subject to pathway annotation analysis. Only cell types with no less than 20 DEGs were included in this analysis. Gene ontology analysis was conducted using clusterprofiler package[85] with *C. elegans* gene ontology biological pathway (GOBP), molecular function (GOMF) database[86] and wormbase phenotype database.[36] Enrichment P values were corrected by Benjamini–Hochberg method and FDR < 0.05 were considered significant, only pathways with more than 2 overlapped genes were kept. For significantly enriched pathways, fold changes were calculated by averaging the fold changes of the pathway genes between treatment and control nuclei. For WormBase phenotypes, we also retrieved higher level categories of each phenotype by querying EBI OLS (ontology lookup service) API. Annotations from top level (nematode phenotype, physiology phenotype and anatomical phenotype) were not used since these terms were too general for interpretations. We further selected top 20 most common annotations and compared their proportion in original database with our enrichment results.

Euclidean distance-based measurement of cell type sensitivity—To identify cell types that are sensitive to ethanol treatment, the Euclidean distance metric was used.[53] For each cell type with more than 10 cells in both ethanol and control group per batch, expression distance between nuclei of water and ethanol treatment groups were squared and summed, followed by taking the square root. In order to avoid potential biases caused by genes that are either highly expressed or non-expressed, expression values were normalized to z-scores and only the top 1,000 expressed genes were used. To account for variabilities in expression characteristics per each cell type, null distributions for individual cell types were calculated based on permutated treatment labels for 1,000 times. P values were calculated between the observed Euclidean distance and the null distribution for each cell type and adjusted with the Benjamini & Hochberg method.[84]

To visualize the differences between water and ethanol treated nuclei for individual cell types, the fold change (FC) in the Euclidean distance of ethanol treatment group compared with water treatment group in each cell type was normalized by dividing the empirical Euclidean distance by the median Euclidean distance of the null distribution per cell type. The log10(FC) vs. −log10(adjusted p value) of each cell type was then plotted to visualize and rank the vulnerable cell types in ethanol treatment. For 0.05% where two batches were generated, FDR and log10(FC) were averaged.

Single molecule fluorescence *in situ* hybridization—Single molecule fluorescence *in situ* hybridization (smFISH) was performed on F1 and F3 adults that were maintained, exposed, and filtered in a similar manner to animals used in the single-nucleus dissociation protocol. smFISH was performed using the protocol developed by the Kimble Lab.[41] Probes were designed and ordered through Stellaris and are compiled in Table S1. All probes were used at a final concentration of 0.25μM with approximately 100 dissected worms per condition. Samples were mounted on slides using fluoroshield with DAPI (Sigma-Aldrich F6057). Slides were imaged on the Leica SP8 confocal microscope. Fluorescence images were quantified using FISH-Quant v3.[80]

Embryonic lethality assessment, *xol-1::*gfp analysis, and apoptosis assay—Embryonic lethality was performed on wild-type N2 F1 and F3 worms. At both generations, L4s were singled out and moved onto individual 33mm plates. Embryonic lethality was performed by monitoring the number of embryos produced each day and the subsequent larvae that hatched from these embryos for each individual worm spanning its entire reproductive lifespan. *Pxol-1::gfp* analysis was done by fluorescent microscopy on 24-hours post-L4 F1 and F3 adults and the occurrence of GFP+ embryos (expressing *Pxol-1::gfp*) was recorded. The proportion of XOL-1::GFP+ was calculated by dividing the number of worms with at least 1 GFP+ embryo by the total number of worms analyzed.[59] Apoptosis assays were performed on wild-type N2 worms by Acridine Orange staining of synchronized adult hermaphrodites collected at 20–24 hours post-L4 at the F1 and F3 generations as previously described.[55,58]

QUANTIFICATION AND STATISTICAL ANALYSIS

All statistical analysis can be found in the respective corresponding figure legend as well as in the “Results” section. Unless otherwise mentioned, statistical analysis was conducted by R/3.5.1.

ADDITIONAL RESOURCES

The data can be accessed and browsed through the Broad Single Cell Portal: https://singlecell.broadinstitute.org/single_cell/study/SCP922/single-nucleus-resolution-mapping-of-the-adult-c-elegans-and-its-application-to-elucidate-inter-and-trans-generational-response-to-alcohol.

Supplementary Material

Refer to Web version on PubMed Central for supplementary material.

ACKNOWLEDGMENTS

The authors would like to thank Doug Arneson for input on single-nucleus sequencing parameters; Ingrid Cely, In Sook Ahn, and Graciel Diamante for discussions and troubleshooting advice; Eyal Ben David for advice on single-cell/-nuclei dissociation methods; Jessica Scholes, Jeffrey Calim, Felicia Codrea, and Salem Haile for guidance with single-nucleus cytometry; Michael Mashock and Marco De Simone for their library preparation and sequencing expertise; the CNSI ALMS (RRID: SCR_022789) for their guidance with advanced microscopy; and Matteo Pellegrini for advice and input on data analysis. We thank Judith Kimble, Tina Lynch, and Sarah Crittenden for advice on smFISH and providing the sygl-1 probe. The *Caenorhabditis* Genetics Center (CGC) (RRID:SCR_007341) provided the strains used in this study. We thank Yuji Kohara for permission to use NEXTDB (RRID:SCR_004480) *in situ* data. Figure 1A and the graphical abstract were created with BioRender.com. L.T. is supported by the NIH Training Grant in Genomic Analysis and Interpretation T32 HG002536; Y.-W.C. is supported by the UCLA Eureka fellowship and Burroughs Wellcome Fund Inter-school Training Program in Chronic Diseases; P.A. is supported by NIEHS R01 ES027487, NIAAA R21 AA024889, the John Templeton Foundation, and the Burroughs Wellcome Innovation in Regulatory Science Award. E.d.V.B. and P.W.S. are supported by U24HG002223.

REFERENCES

1. Denny L, Coles S, and Blitz R (2017). Fetal alcohol syndrome and fetal alcohol spectrum disorders. Am. Fam. Physician 96, 515–522. [PubMed: 29094891]
2. Caputo C, Wood E, and Jabbour L (2016). Impact of fetal alcohol exposure on body systems: a systematic review. Birth Defects Res. C Embryo Today. 108, 174–180. 10.1002/bdrc.21129. [PubMed: 27297122]
3. La Vignera S, Condorelli RA, Balercia G, Vicari E, and Calogero AE(2013). Does alcohol have any effect on male reproductive function? A review of literature. Asian J. Androl. 15, 221–225. 10.1038/aja.2012.118. [PubMed: 23274392]
4. Strategic plan 2017–2021. https://www.niaaa.nih.gov/strategic-plan.
5. Abbott CW, Rohac DJ, Bottom RT, Patadia S, and Huffman KJ(2018). Prenatal ethanol exposure and neocortical development: a transgenerational model of FASD. Cereb. Cortex 28, 2908–2921. 10.1093/cercor/bhx168. [PubMed: 29106518]
6. Bozler J, Kacsoh BZ, and Bosco G (2019). Transgeneratonal inheritance of ethanol preference is caused by maternal NPF repression. Elife 8, e45391. 10.7554/eLife.45391. [PubMed: 31287057]
7. Gangisetty O, Palagani A, and Sarkar DK (2020). Transgenerational inheritance of fetal alcohol exposure adverse effects on immune gene interferon-Y. Clin. Epigenetics 12, 70. 10.1186/s13148-020-00859-9. [PubMed: 32448218]
8. Bottom RT, Kozanian OO, Rohac DJ, Erickson MA, and Huffman KJ (2022). Transgenerational effects of prenatal ethanol exposure in prepubescent mice. Front. Cell Dev. Biol. 10, 812429. 10.3389/fcell.2022.812429. [PubMed: 35386207]
9. Nizhnikov ME, Popoola DO, and Cameron NM (2016). Transgenerational transmission of the effect of gestational ethanol exposure on ethanol use-related behavior. Alcohol Clin. Exp. Res. 40, 497–506. 10.1111/acer.12978. [PubMed: 26876534]
10. Gangisetty O, Chaudhary S, Palagani A, and Sarkar DK (2022). Transgenerational inheritance of fetal alcohol effects on proopiomelanocortin gene expression and methylation, cortisol response to stress, and anxiety-like behaviors in offspring for three generations in rats: evidence for male germline transmission. PLoS One 17, e0263340. 10.1371/journal.pone.0263340. [PubMed: 35143549]
11. Lam MK, Homewood J, Taylor AJ, and Mazurski EJ (2000). Second-generation effects of maternal alcohol consumption during pregnancy in rats. Prog. Neuro-Psychopharmacol. Biol. Psychiatry 24, 619–631. 10.1016/S0278-5846(00)00097-X.
12. Yohn NL, Bartolomei MS, and Blendy JA (2015). Multigenerational and transgenerational inheritance of drug exposure: the effects of alcohol, opiates, cocaine, marijuana, and nicotine. Prog. Biophys. Mol. Biol. 118, 21–33. 10.1016/j.pbiomolbio.2015.03.002. [PubMed: 25839742]
13. Patten AR, Fontaine CJ, and Christie BR (2014). A comparison of the different animal models of fetal alcohol spectrum disorders and their use in studying complex behaviors. Front. Pediatr. 2, 93. 10.3389/fped.2014.00093. [PubMed: 25232537]

14. Mitchell PH, Bull K, Glautier S, Hopper NA, Holden-Dye L, and O'Connor V (2007). The concentration-dependent effects of ethanol on Caenorhabditis elegans behaviour. Pharmacogenomics J. 7, 411–417. 10.1038/sj.tpj.6500440. [PubMed: 17325734]
15. Lee J, Jee C, and McIntire SL (2009). Ethanol preference in C. elegans. Genes Brain Behav. 8, 578–585. 10.1111/j.1601-183X.2009.00513.x. [PubMed: 19614755]
16. McIntire SL (2010). Ethanol. WormBook, 1–6. 10.1895/wormbook.1.40.1.
17. Topper SM, Aguilar SC, Topper VY, Elbel E, and Pierce-Shimomura JT (2014). Alcohol disinhibition of behaviors in C. elegans. PLoS One 9, e92965. 10.1371/journal.pone.0092965. [PubMed: 24681782]
18. Pandey P, Singh A, Kaur H, Ghosh-Roy A, and Babu K (2021). Increased dopaminergic neurotransmission results in ethanol dependent sedative behaviors in Caenorhabditis elegans. PLoS Genet. 17, e1009346. 10.1371/journal.pgen.1009346. [PubMed: 33524034]
19. Alaimo JT, Davis SJ, Song SS, Burnette CR, Grotewiel M, Shelton KL, Pierce-Shimomura JT, Davies AG, and Bettinger JC (2012). Ethanol metabolism and osmolarity modify behavioral responses to ethanol in C. elegans. Alcohol Clin. Exp. Res. 36, 1840–1850. 10.1111/j.1530-0277.2012.01799.x. [PubMed: 22486589]
20. Cao J, Packer JS, Ramani V, Cusanovich DA, Huynh C, Daza R,Qiu X, Lee C, Furlan SN, Steemers FJ, et al. (2017). Comprehensive single-cell transcriptional profiling of a multicellular organism. Science 357, 661–667. 10.1126/science.aam8940. [PubMed: 28818938]
21. Packer JS, Zhu Q, Huynh C, Sivaramakrishnan P, Preston E, Dueck H, Stefanik D, Tan K, Trapnell C, Kim J, et al. (2019). A lineage-resolved molecular atlas of C. elegans embryogenesis at single-cell resolution. Science 365, eaax1971. 10.1126/science.aax1971. [PubMed: 31488706]
22. Taylor SR, Santpere G, Weinreb A, Barrett A, Reilly MB, Xu C, Varol E, Oikonomou P, Glenwinkel L, McWhirter R, et al. (2021). Molecular topography of an entire nervous system. Cell 184, 4329–4347.e23. 10.1016/j.cell.2021.06.023. [PubMed: 34237253]
23. Camacho J, and Allard P (2018). Histone modifications: epigenetic mediators of environmental exposure memory. Epigenet. Insights 11. 2516865718803641. [PubMed: 30443644]
24. Weinhouse C, Truong L, Meyer JN, and Allard P (2018). Caenorhabditis elegans as an emerging model system in environmental epigenetics. Environ. Mol. Mutagen. 59, 560–575. 10.1002/em.22203. [PubMed: 30091255]
25. Camacho J, Truong L, Kurt Z, Chen Y-W, Morselli M, Gutierrez G, Pellegrini M, Yang X, and Allard P (2018). The memory of environmental chemical exposure in C. elegans is dependent on the Jumonji demethylases jmjd-2 and jmjd-3/utx-1. Cell Rep. 23, 2392–2404. 10.1016/j.celrep.2018.04.078. [PubMed: 29791850]
26. Kelly WG (2014). Transgenerational epigenetics in the germline cycle of Caenorhabditis elegans. Epigenet. Chromatin 7, 6. 10.1186/1756-8935-7-6.
27. Kishimoto S, Uno M, Okabe E, Nono M, and Nishida E (2017). Environmental stresses induce transgenerationally inheritable survival advantages via germline-to-soma communication in Caenorhabditis elegans. Nat. Commun. 8, 14031. 10.1038/ncomms14031. [PubMed: 28067237]
28. Klosin A, Casas E, Hidalgo-Carcedo C, Vavouri T, and Lehner B(2017).Transgenerational transmission of environmental information in C. elegans. Science 356, 320–323. 10.1126/science.aah6412. [PubMed: 28428426]
29. Podbilewicz B (2006). Cell fusion. WormBook 1–32, 1–32. 10.1895/wormbook.1.52.1.
30. Amini R, Chartier NT, and Labbé JC (2015). Syncytium biogenesis: it's all about maintaining good connections. Worm 4, e992665. 10.4161/21624054.2014.992665. [PubMed: 26430559]
31. Barton MK, and Kimble J (1990). fog-1, a regulatory gene required for specification of spermatogenesis in the germ line of Caenorhabditis elegans. Genetics.
32. Alvarez M, Rahmani E, Jew B, Garske KM, Miao Z, Benhammou JN, Ye CJ, Pisegna JR, Pietiläinen KH, Halperin E, and Pajukanta P (2020). Enhancing droplet-based single-nucleus RNA-seq resolution using the semi-supervised machine learning classifier DIEM. Sci. Rep. 10, 11019. 10.1038/s41598-020-67513-5. [PubMed: 32620816]
33. Young MD, and Behjati S (2020). SoupX removes ambient RNA contamination from droplet-based single-cell RNA sequencing data. Gig-aScience 9, giaa151. 10.1093/gigascience/giaa151.

34. Stuart T, Butler A, Hoffman P, Hafemeister C, Papalexi E, Mauck WM, Hao Y, Stoeckius M, Smibert P, and Satija R (2019). Comprehensive integration of single-cell data. Cell 177, 1888–1902.e21. 10.1016/j.cell.2019.05.031. [PubMed: 31178118]
35. Waltman L, and Van Eck NJ (2013). A smart local moving algorithm for large-scale modularity-based community detection. Eur. Phys. J. B 86, 471. 10.1140/epjb/e2013-40829-0.
36. Angeles-Albores D, N Lee RY, Chan J, and Sternberg PW (2016). Tissue enrichment analysis for C. elegans genomics. BMC Bioinf. 17, 366. 10.1186/s12859-016-1229-9.
37. Hu S, Skelly LE, Kaymak E, Freeberg L, Lo T-W, Kuersten S, Ryder SP, and Haag ES (2019). Multi-modal regulation of C. elegans hermaphrodite spermatogenesis by the GLD-1-FOG-2 complex. Dev. Biol. 446, 193–205. 10.1016/j.ydbio.2018.11.024. [PubMed: 30599151]
38. Dernburg AF, McDonald K, Moulder G, Barstead R, Dresser M, and Villeneuve AM (1998). Meiotic recombination in C. elegans initiates by a conserved mechanism and is dispensable for homologous chromosome synapsis. Cell 94, 387–398. 10.1016/S0092-8674(00)81481-6. [PubMed: 9708740]
39. Colaiácovo MP (2006). The many facets of SC function during C. elegans meiosis. Chromosoma 115, 195–211. 10.1007/s00412-006-0061-9. [PubMed: 16555015]
40. Shin H, Haupt KA, Kershner AM, Kroll-Conner P, Wickens M, and Kimble J (2017). SYGL-1 and LST-1 link niche signaling to PUF RNA repression for stem cell maintenance in Caenorhabditis elegans. PLoS Genet. 13, e1007121. 10.1371/journal.pgen.1007121. [PubMed: 29232700]
41. Lee C, Seidel HS, Lynch TR, Sorensen EB, Crittenden SL, and Kimble J (2017). Single-molecule RNA fluorescence in situ hybridization (smFISH) in Caenorhabditis elegans. Bio. Protoc. 7, e2357. 10.21769/BioProtoc.2357.
42. Gissendanner CR, Kelley K, Nguyen TQ, Hoener MC, Sluder AE, and Maina CV (2008). The Caenorhabditis elegans NR4A nuclear receptor is required for spermatheca morphogenesis. Dev. Biol. 313, 767–786. 10.1016/j.ydbio.2007.11.014. [PubMed: 18096150]
43. Kalis AK, Kroetz MB, Larson KM, and Zarkower D (2010). Functional genomic identification of genes required for male gonadal differentiation in Caenorhabditis elegans. Genetics 185, 523–535. 10.1534/genetics.110.116038. [PubMed: 20308279]
44. Jorgensen EM (2005). Gaba. WormBook, 1–13. 10.1895/wormbook.1.14.1.
45. Rand J (2007). Acetylcholine. WormBook 1, 1–21. 10.1895/wormbook.1.131.1.
46. Martinez-Hurtado J, Calo-Fernandez B, and Vazquez-Padin J (2018). Preventing and mitigating alcohol toxicity: a review on protective substances. Beverages 4, 39. 10.3390/beverages4020039.
47. David ET, Fischer I, and Moldave K (1983). Studies on the effect of ethanol on eukaryotic protein synthesis in vitro. J. Biol. Chem. 258, 7702–7706. 10.1016/s0021-9258(18)32236-1. [PubMed: 6553051]
48. Cahill A, Baio DL, Ivester P, and Cunningham CC (1996). Differential effects of chronic ethanol consumption on hepatic mitochondrial and cytoplasmic ribosomes. Alcohol Clin. Exp. Res. 20, 1362–1367. 10.1111/j.1530-0277.1996.tb01135.x. [PubMed: 8947311]
49. Vary TC, Lynch CJ, and Lang CH (2001). Effects of chronic alcohol consumption on regulation of myocardial protein synthesis. Am. J. Physiol. Heart Circ. Physiol. 281, H1242–H1251. 10.1152/ajpheart.2001.281.3.H1242. [PubMed: 11514293]
50. Karinch AM, Martin JH, and Vary TC (2008). Acute and chronic ethanol consumption differentially impact pathways limiting hepatic protein synthesis. Am. J. Physiol. Endocrinol. Metab. 295, E3–E9. 10.1152/ajpendo.00026.2008. [PubMed: 18334613]
51. Haft RJF, Keating DH, Schwaegler T, Schwalbach MS, Vinokur J, Tremaine M, Peters JM, Kotlajich MV, Pohlmann EL, Ong IM, et al. (2014). Correcting direct effects of ethanol on translation and transcription machinery confers ethanol tolerance in bacteria. Proc. Natl. Acad. Sci. USA 111, E2576–E2585. 10.1073/pnas.1401853111. [PubMed: 24927582]
52. Berres ME, Garic A, Flentke GR, and Smith SM (2017). Transcriptome profiling identifies ribosome biogenesis as a target of alcohol teratogenicity and vulnerability during early embryogenesis. PLoS One 12, e0169351. 10.1371/journal.pone.0169351. [PubMed: 28046103]
53. Arneson D, Zhang G, Ying Z, Zhuang Y, Byun HR, Ahn IS, Gomez-Pinilla F, and Yang X (2018). Single cell molecular alterations reveal target cells and pathways of concussive brain injury. Nat. Commun. 9, 3894. 10.1038/s41467-018-06222-0. [PubMed: 30254269]

54. Liu W, Venugopal S, Majid S, Ahn IS, Diamante G, Hong J, Yang X, and Chandler SH (2020). Single-cell RNA-seq analysis of the brain-stem of mutant SOD1 mice reveals perturbed cell types and pathways of amyotrophic lateral sclerosis. Neurobiol. Dis. 141, 104877. 10.1016/j.nbd.2020.104877. [PubMed: 32360664]
55. Gartner A, Boag PR, and Blackwell TK (2008). Germline survival and apoptosis. WormBook, 1–20. 10.1895/wormbook.1.145.1.
56. Nicoll M, Akerib CC, and Meyer BJ (1997). X-chromosome-counting mechanisms that determine nematode sex. Nature 388, 200–204. 10.1038/40669. [PubMed: 9217163]
57. MacQueen AJ, Colaiácovo MP, McDonald K, and Villeneuve AM (2002). Synapsis-dependent and -independent mechanisms stabilize homolog pairing during meiotic prophase in C. elegans. Genes Dev. 16, 2428–2442. 10.1101/gad.1011602. [PubMed: 12231631]
58. Chen Y, Shu L, Qiu Z, Lee DY, Settle SJ, Que Hee S, Telesca D, Yang X, and Allard P (2016). Exposure to the BPA-substitute Bisphenol S causes unique alterations of germline function. PLoS Genet. 12, e1006223. 10.1371/journal.pgen.1006223. [PubMed: 27472198]
59. Allard P, Kleinstreuer NC, Knudsen TB, and Colaiácovo MP (2013). A screening platform for the rapid assessment of chemical disruption of germline function. Environ. Health Perspect. 121, 717–724. 10.1289/ehp.1206301. [PubMed: 23603051]
60. Urbano-Marquez A, Estruch R, Navarro-Lopez F, Grau JM, Mont L, and Rubin E (1989). The effects of alcoholism on skeletal and cardiac muscle. N. Engl. J. Med. 320, 409–415. 10.1056/NEJM198902163200701. [PubMed: 2913506]
61. Meehan J, Piano MR, Solaro RJ, and Kennedy JM (1999). Heavy long-term ethanol consumption induces an alpha- to beta-myosin heavy chain isoform transition in rat. Basic Res. Cardiol. 94, 481–488. 10.1007/s003950050164. [PubMed: 10651160]
62. Hunter RJ, Neagoe C, Järveläinen HA, Martin CR, Lindros KO, Linke WA, and Preedy VR (2003). Alcohol affects the skeletal muscle proteins, titin and nebulin in male and female rats. J. Nutr. 133, 1154–1157. 10.1093/jn/133.4.1154. [PubMed: 12672935]
63. David P, and Subramaniam K (2005). Prenatal alcohol exposure and early postnatal changes in the developing nerve-muscle system. Birth Defects Res. A Clin. Mol. Teratol. 73, 897–903. 10.1002/bdra.20190. [PubMed: 16228975]
64. Myrie SB, and Pinder MA (2018). Skeletal muscle and fetal alcohol spectrum disorder. Biochem. Cell. Biol. 96, 222–229. 10.1139/bcb-2017-0118. [PubMed: 29091741]
65. Davis TA, and Fiorotto ML (2009). Regulation of muscle growth in neonates. Curr. Opin. Clin. Nutr. Metab. Care 12, 78–85. 10.1097/MCO.0b013e32831cef9f. [PubMed: 19057192]
66. Lin G, Wang X, Wu G, Feng C, Zhou H, Li D, and Wang J (2014). Improving amino acid nutrition to prevent intrauterine growth restriction in mammals. Amino Acids 46, 1605–1623. 10.1007/s00726-014-1725-z. [PubMed: 24658999]
67. Olney JW, Wozniak DF, Jevtovic-Todorovic V, Farber NB, Bittigau P, and Ikonomidou C (2002). Glutamate and GABA receptor dysfunction in the fetal alcohol syndrome. Neurotox. Res. 4, 315–325. 10.1080/1029842021000010875. [PubMed: 12829421]
68. Davies M (2003). The role of GABAA receptors in mediating the effects of alcohol in the central nervous system. J. Psychiatry Neurosci. 28, 263–274. [PubMed: 12921221]
69. Lobo IA, and Harris RA (2008). GABA(A) receptors and alcohol. Pharmacol.Biochem.Behav.90,90–94.10.1016/j.pbb.2008.03.006. [PubMed: 18423561]
70. Smiley JF, Saito M, Bleiwas C, Masiello K, Ardekani B, Guilfoyle DN, Gerum S, Wilson DA, and Vadasz C (2015). Selective reduction of cerebral cortex GABA neurons in a late gestation model of fetal alcohol spectrum disorder. Alcohol 49, 571–580. 10.1016/j.alcohol.2015.04.008. [PubMed: 26252988]
71. Wozniak JR, Fink BA, Fuglestad AJ, Eckerle JK, Boys CJ, Sandness KE, Radke JP, Miller NC, Lindgren C, Brearley AM, et al. (2020). Four-year follow-up of a randomized controlled trial of choline for neurodevelopment in fetal alcohol spectrum disorder. J. Neurodev. Disord. 12, 9. 10.1186/s11689-020-09312-7. [PubMed: 32164522]
72. Milbocker KA, and Klintsova AY (2021). Examination of cortically projecting cholinergic neurons following exercise and environmental intervention in a rodent model of fetal alcohol spectrum disorders. Birth Defects Res. 113, 299–313. 10.1002/bdr2.1839. [PubMed: 33174398]

73. Macht VA, Vetreno RP, and Crews FT (2022). Cholinergic and neuroimmune signaling interact to impact adult hippocampal neurogenesis and alcohol pathology across development. Front. Pharmacol. 13, 849997. 10.3389/fphar.2022.849997. [PubMed: 35308225]
74. Hawkins EG, Martin I, Kondo LM, Judy ME, Brings VE, Chan C-L, Blackwell GG, Bettinger JC, and Davies AG (2015). A novel cholinergic action of alcohol and the development of tolerance to that effect in Caenorhabditis elegans. Genetics 199, 135–149. 10.1534/genetics.114.171884. [PubMed: 25342716]
75. Kaufman MH (1983). Ethanol-induced chromosomal abnormalities at conception. Nature 302, 258–260. 10.1038/302258a0. [PubMed: 6682181]
76. Kaufman MH, and Bain IM (1984). Influence of ethanol on chromosome segregation during the first and second meiotic divisions in the mouse egg. J. Exp. Zool. 230, 315–320. 10.1002/jez.1402300217. [PubMed: 6429271]
77. Shi Q, and Martin RH (2000). Aneuploidy in human sperm: a review of the frequency and distribution of aneuploidy, effects of donor age and lifestyle factors. Cytogenet. Cell Genet. 90, 219–226. [PubMed: 11124518]
78. Mews P, Egervari G, Nativio R, Sidoli S, Donahue G, Lombroso SI, Alexander DC, Riesche SL, Heller EA, Nestler EJ, et al. (2019). Alcohol metabolism contributes to brain histone acetylation. Nature 574, 717–721. 10.1038/s41586-019-1700-7. [PubMed: 31645761]
79. Hobert O, Glenwinkel L, and White J (2016). Revisiting neuronal cell type classification in Caenorhabditis elegans. Curr. Biol. 26, R1197–R1203. 10.1016/j.cub.2016.10.027. [PubMed: 27875702]
80. Mueller F, Senecal A, Tantale K, Marie-Nelly H, Ly N, Collin O, Basyuk E, Bertrand E, Darzacq X, and Zimmer C (2013). FISH-quant: automatic counting of transcripts in 3D FISH images. Nat. Methods 10, 277–278. 10.1038/nmeth.2406. [PubMed: 23538861]
81. Macosko EZ, Basu A, Satija R, Nemesh J, Shekhar K, Goldman M, Tirosh I, Bialas AR, Kamitaki N, Martersteck EM, et al. (2015). Highly Parallel genome-wide expression profiling of individual cells using nanoliter droplets. Cell 161, 1202–1214. 10.1016/j.cell.2015.05.002. [PubMed: 26000488]
82. Haynes W (2013). Wilcoxon rank Sum test. In Encyclopedia of Systems Biology (Springer), pp. 2354–2355. 10.1007/978-1-44199863-7_1185.
83. Qiu X, Hill A, Packer J, Lin D, Ma Y-A, and Trapnell C (2017). Single-cell mRNA quantification and differential analysis with Census. Nat. Methods 14, 309–315. 10.1038/nmeth.4150. [PubMed: 28114287]
84. Benjamini Y, and Hochberg Y (1995). Controlling the false discovery rate: a practical and powerful approach to multiple testing. J. R. Stat. Soc. Series B Stat. Methodol. 57, 289–300. 10.1111/j.2517-6161.1995.tb02031.x.
85. Yu G, Wang L-G, Han Y, and He Q-Y (2012). clusterProfiler: an R package for comparing biological themes among gene clusters. OMICS 16, 284–287. 10.1089/omi.2011.0118. [PubMed: 22455463]
86. The Gene Ontology Consortium (2017). Expansion of the gene ontology knowledgebase and resources. Nucleic Acids Res. 45, D331–D338. 10.1093/nar/gkw1108. [PubMed: 27899567]

Highlights

- Single-nucleus RNA-seq was used to profile the transcriptome of the adult *C. elegans*
- This approach captured the transcriptome of syncytial tissues such as the germline
- snRNA-seq was applied to assess ethanol's inter- and trans-generational effects
- Ethanol transcriptionally and functionally impacts germline homeostasis

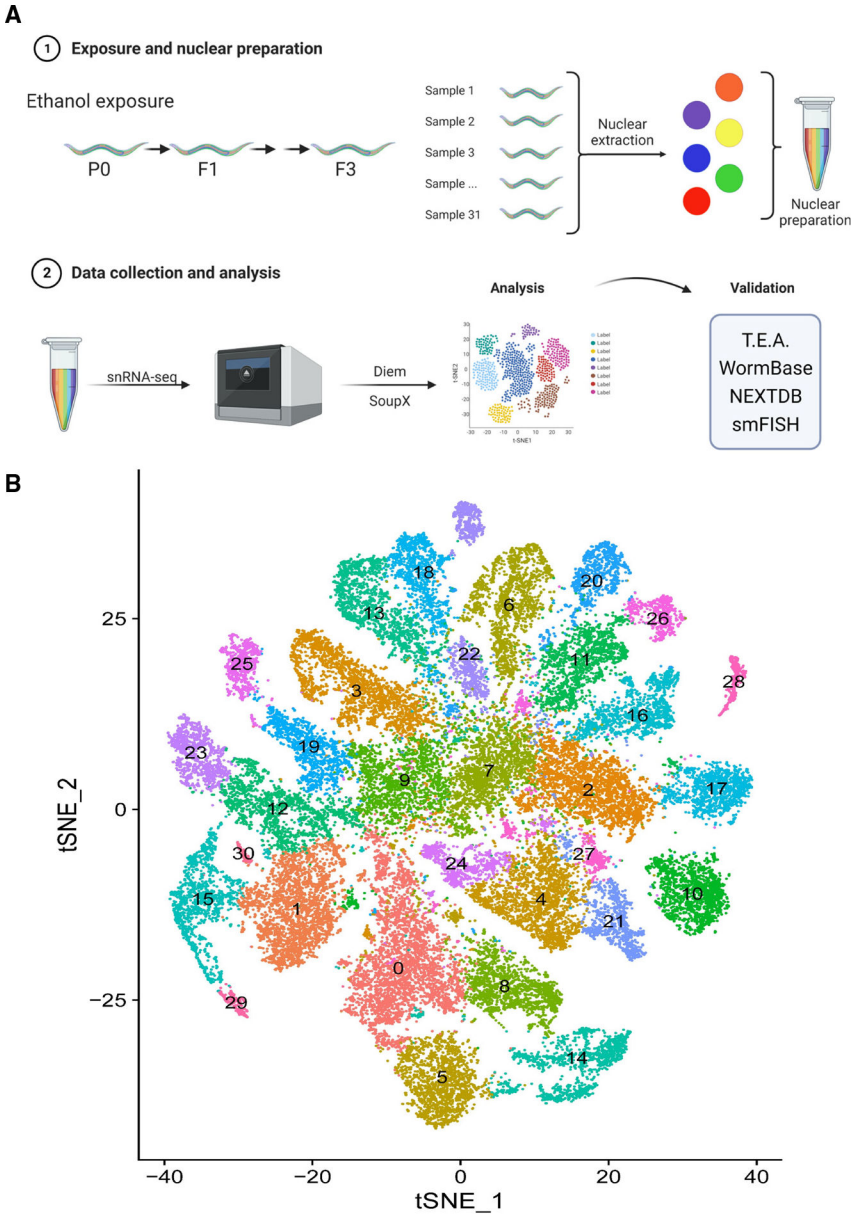

Figure 1. Adult *C. elegans* snRNA-seq sample preparation, analysis, and t-SNE projection

(A) Experimental flow for single-nucleus isolation and snRNA-seq analysis.

(B) t-SNE plot of cells from all the samples with clustering through unsupervised Louvain clustering. Cluster molecular characterization and identity is presented in the corresponding dashboard (Data S2).

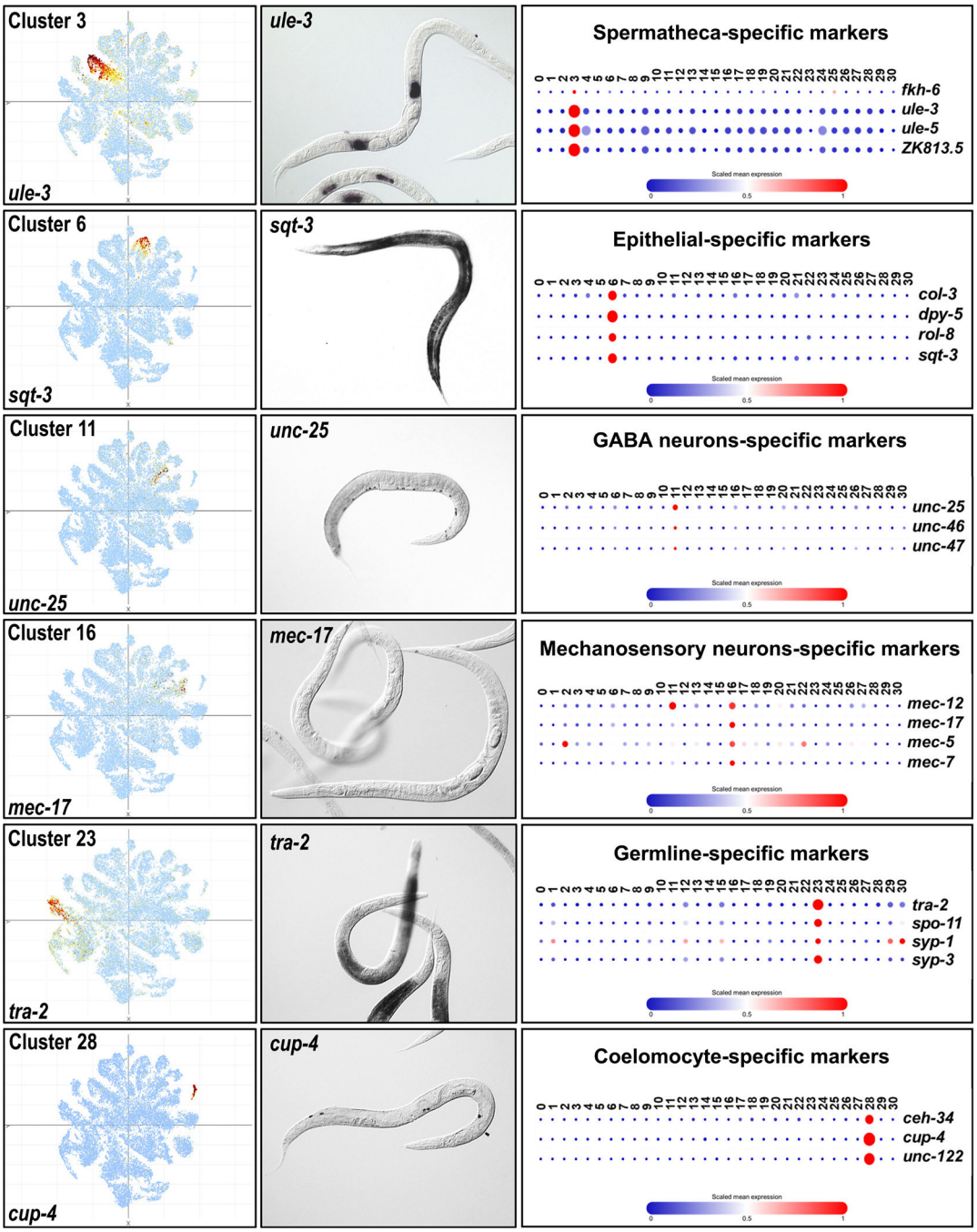

Figure 2. Cluster-resolved expression of cell type-specific markers

Example of cluster-specific expression of cell type specific markers for the spermatheca, epithelial cells, GABA and mechanosensory neurons, germline, and coelomocyte. Left column: cluster-specific expression. Middle column: representative *in situ* expression data from NEXTDB for corresponding marker. Right column: gene expression dot plot of known cell type-specific markers.

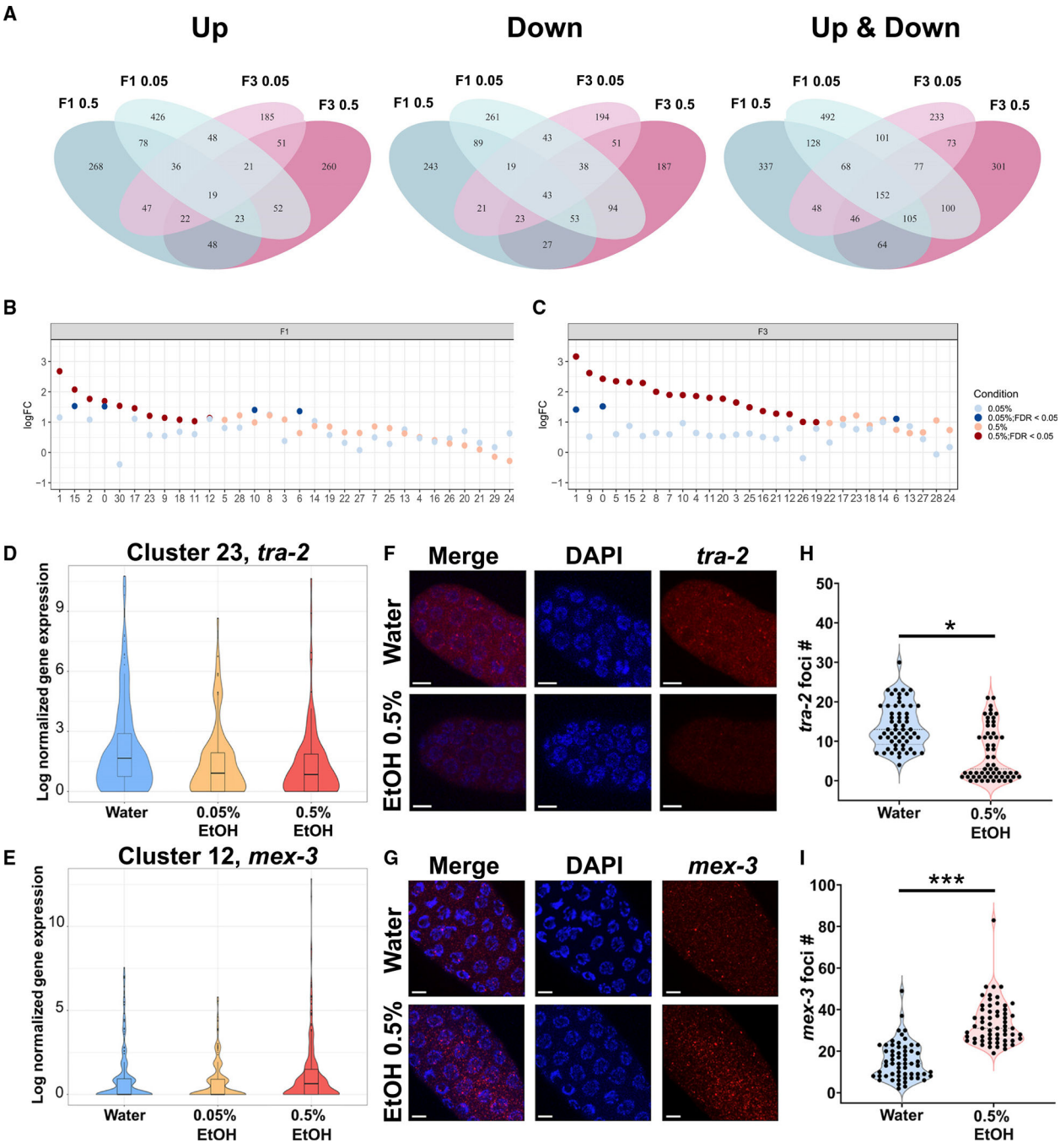

Figure 3. Global and cluster-specific alterations in gene expression by inter- or trans-generational ethanol exposure

(A) Venn diagram based on the union of DEGs across all the cell types, separated by upregulated DEGs only (left), downregulated genes only (middle), and all DEGs (right). (B and C) Euclidean distance sensitivity analysis of all the cell clusters at the F1 generation (B) or F3 generation (C). The x axis indicates cluster number and the y axis indicates log fold change compared with the Euclidean distance obtained by permuting treatment labels. Significance was assessed based on comparing Euclidean distance against 1,000 random permutated labels.

(D and E) Expression of *tra-2* in cluster 23 at the F1 (D) and *mex-3* in cluster 12 at the F3 (E).

(F–I) Validation of snRNA-seq data through single-molecule fluorescence *in situ* hybridization (smFISH) by confocal imaging (F and G) followed by FISH-quant (H and I). Scale bar: 5 μm. 3 biological replicates, 2 worms per repeat, 10 nuclei per germline. *$p < 0.05$, ***$p < 0.001$. Welch's t test.

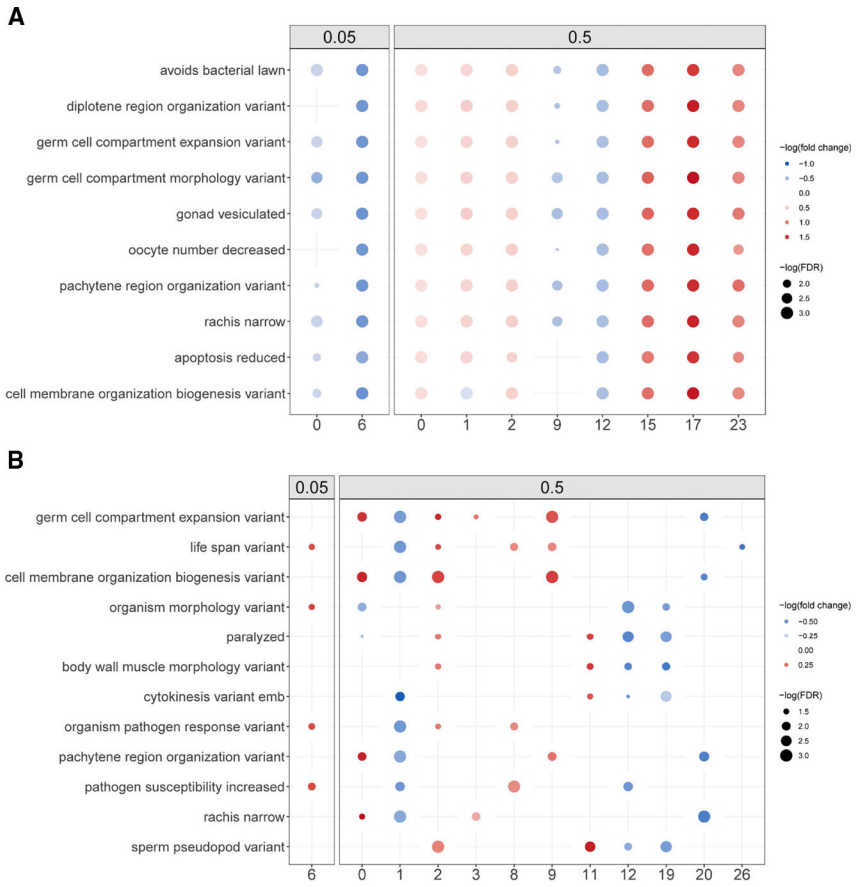

Figure 4. Wormbase phenotypes shared across cell types in response to inter- or trans-generational ethanol exposure

Dot heatmap of top WormBase phenotype shared across cell types with significantly altered Euclidean distance metrics at the F1 (A) or F3 (B). Dot size corresponds to −log(FDR) obtained from enrichment analysis, and dot color corresponds to −log(median fold change) of overlapping genes in each pathway.

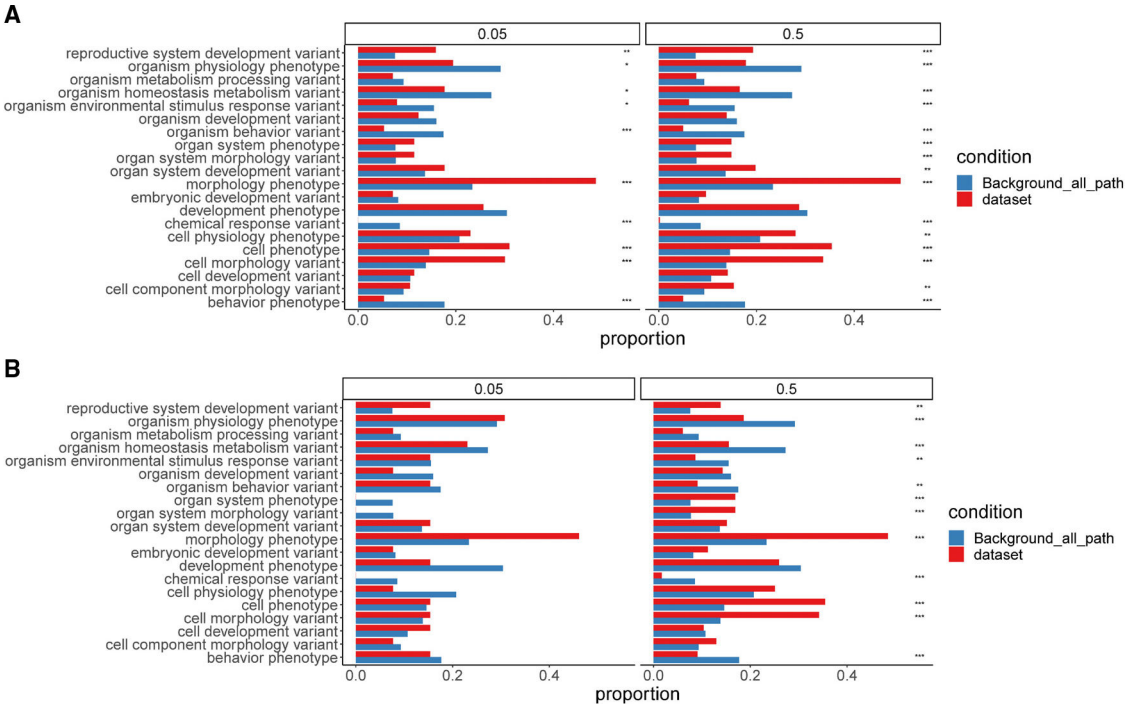

Figure 5. WormBase phenotype annotation enrichment in response to inter- or trans-generational ethanol exposure

Bar plot showing the proportion of top WormBase phenotype annotations from all enriched pathways (“dataset”) and WormBase phenotype database (“Background_all_path”) at the F1 (A) or F3 (B). For each WormBase phenotype from the original database, we retrieved the corresponding WormBase phenotype annotations by querying EBI OLS API, followed by selecting the top 20 shared phenotypes. Proportions were calculated based on the proportion of annotations among all enriched pathways (“dataset”) and the WormBase phenotype database (“Background_all_path”). Fisher’s exact test was used to compare proportions between the two conditions in each annotation category.

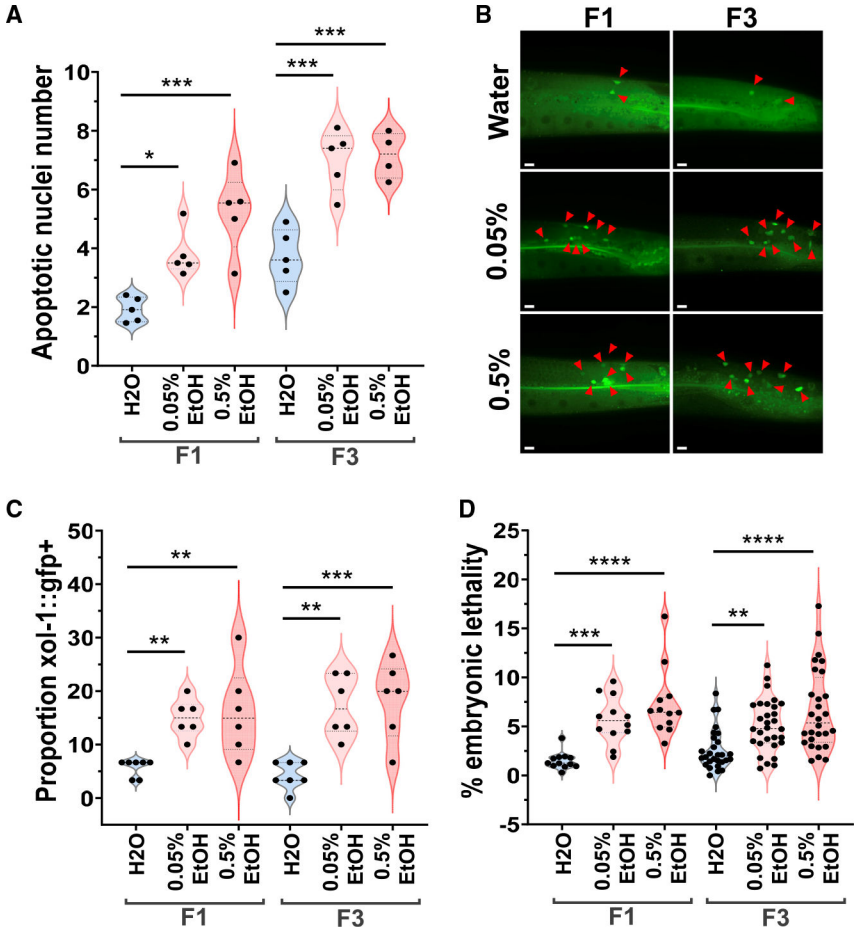

Figure 6. P0 ethanol exposure causes reproductive dysfunction at the F1 and F3 generations

P0 hermaphrodites were exposed to water, 0.05% ethanol, or 0.5% ethanol.

(A and B) Number of apoptotic nuclei per gonadal arm in N2 worms at the F1 and F3 exposed to the indicated ethanol levels, n = 4–5, 22 worms per repeat. Scale bars: 10 μm.

(C) Assessment of errors of X chromosome segregation as measured by *Pxol-1::gfp* reporter. Out of 30 worms per repeat, the percentage (%) of worms with at least 1 GFP+ embryo was recorded, n = 6, 30 worms per repeat.

(D) Percentage of embryonic lethality per worm was measured for N2, n = 4–10, 2–3 worms per repeat. One-way ANOVA with Dunnett correction. *p < 0.05, **p < 0.01, ***p < 0.001, ****p < 0.0001.

Table 1.

Shared pathways identified through DEG analysis across both exposures and generations

Pathway	Generation/condition
Peptide metabolic process	F105, F305, F1005, F3005
Carboxylic acid metabolic process	F105, F305, F1005, F3005
Small molecule biosynthetic process	F105, F305, F1005, F3005
Defense response	F105, F305, F1005, F3005
Translation	F105, F305, F1005
Embryo development ending in birth or egg hatching	F105, F305, F1005
Aging	F105, F1005, F3005
Ribosomal large subunit biogenesis	F105, F305, F1005
Ribosome assembly	F105, F305, F1005
Cytoskeleton organization	F105, F305, F3005
Multi-organism process	F105, F305, F1005
Ribose phosphate metabolic process	F105, F305, F1005
Cellular process involved in reproduction in multicellular organism	F105, F305, F1005
Actin cytoskeleton organization	F105, F305, F3005
Protein catabolic process	F105, F1005, F3005
Response to heat	F105, F305, F1005
Multicellular organismal movement	F105, F305, F3005
rRNA binding	F105, F305, F1005
Phosphotransferase activity, phosphate group as acceptor	F105, F305, F1005
Threonine-type endopeptidase activity	F105, F305, F1005

Top 20 shared pathways identified by the union of all cell type-specific DEGs across the four conditions. F105, 0.5% ethanol exposure at the F1 generation; F1005, 0.05% ethanol exposure at the F1 generation; F305, 0.5% ethanol exposure at the F3 generation; F3005, 0.05% ethanol exposure at the F3 generation.

KEY RESOURCES TABLE

REAGENT or RESOURCE	SOURCE	IDENTIFIER
Chemicals, peptides, and recombinant proteins		
RNase Free Water	Fisher Scientific	# BP2484100
RNase Zap	Fisher Scientific	# AM9780
RNase Inhibitor	Thermo Fisher	# 10777019
Protease Inhibitor	Roche	# 11697498001
Bovine Serum Albumin (BSA)	Fisher Scientific	# BP1600–100
PBS 10X RNase free pH 7.4	Thermo Fisher	# AM9624
HEPES 1M (Gibco)	Thermo Fisher	#15630080
EDTA 0.5M, pH 8.0 (Invitrogen)	Thermo Fisher	#AM9260G
Triton X-100	Fisher Scientific	#BP151–100
Sodium Chloride	Fisher Scientific	S671
70% Ethanol	Fisher Scientific	# 64-17-5
DAPI	Sigma Aldrich	# 10236276001
Sodium Hydroxide (NaOH)	Fisher Scientific	# BP359–500
Hypochlorite (Clorox concentrated bleach)	Fisher Scientific	#50371500
Acridine Orange	Thermo Fisher	#A1301
Deposited data		
Raw snRNA-seq repository	This paper	https://www.ncbi.nlm.nih.gov/geo/query/acc.cgi?acc=GSE208229; GEO:GSE208229
Alternate snRNA-seq repository	This paper	https://singlecell.broadinstitute.org/single_cell/study/SCP922/single-nucleus-resolution-mapping-of-the-adult-c-elegans-and-its-application-to-elucidate-inter-and-trans-generational-response-to-alcohol
Experimental models: Organisms/strains		
C. elegans strain: JK560 [*fog-1(q253)*I.]	*Caenorhabditis* Genetics Center (CGC)	https://cgc.umn.edu/strain/JK560; RRID:WB-STRAIN:WBStrain00022517
C. elegans strain: N2	*Caenorhabditis* Genetics Center (CGC)	https://cgc.umn.edu/strain/N2; RRID:WB-STRAIN:WBStrain00000001
C. elegans strain: TY2431 [him-8(e1489) IV; yIs34 V.]	*Caenorhabditis* Genetics Center (CGC)	https://cgc.umn.edu/strain/TY2431; RRID:WB-STRAIN:WBStrain00035137

REAGENT or RESOURCE	SOURCE	IDENTIFIER
Oligonucleotides		
Probes for smFISH, see Table S1	This paper	N/A
Software and algorithms		
Debris Identification using Expectant Maximization (DIEM)	Alvarez et al.[32]	https://github.com/marcalva/diem
SoupX	Young et al.,[33]	https://github.com/constantAmateur/SoupX
Leica LASX	Leica	https://www.leica-microsystems.com/products/microscope-software/p/leica-las-x-ls/
Fish-Quant V.3	Mueller et al.[80]	https://bitbucket.org/muellerflorian/fish_quant/src/master/
Other		
1.5mL Low Retention tubes (RNase free)	Thermo Fisher	#3448
11.0 μM pore size, hydrophilic nylon filters	EDM Millipore	# NY1102500
Swinnex Filter Holder, 25mm	EDM Millipore	# SX00025000
15mL RNase free tubes	VWR	# 76176–950
50mL RNase free tubes	VWR	# 76176–952
Kimwipes	Fisher Scientific	# 06–666
10μL Pipette Tips, Low bind	Genesee Scientific	# 23–201
200μL Pipette Tips, Low bind	Genesee Scientific	#23–412
1000μL Pipette Tips, Low bind	Genesee Scientific	# 23–430
Flowmi 40μm filters	Sigma Aldrich	# BAH136800040–50EA
DWK Life Sciences Wheaton Dounce Tissue Grinder	Fisher Scientific	# 06–43
10mL Plastic Pipette	Bioland	# 327001
96 well flat-bottom plates	Genesee Scientific	# 25–104
5mL Round-Bottom tube with cell-strainer cap	Falcon	#352235
All-plastic disposable syringes, 50mL	Thermo Fisher	#S7515
Millex-GP 0.22μm syringe filter, gamma sterilized	Millipore Sigma	# SLGP033RS